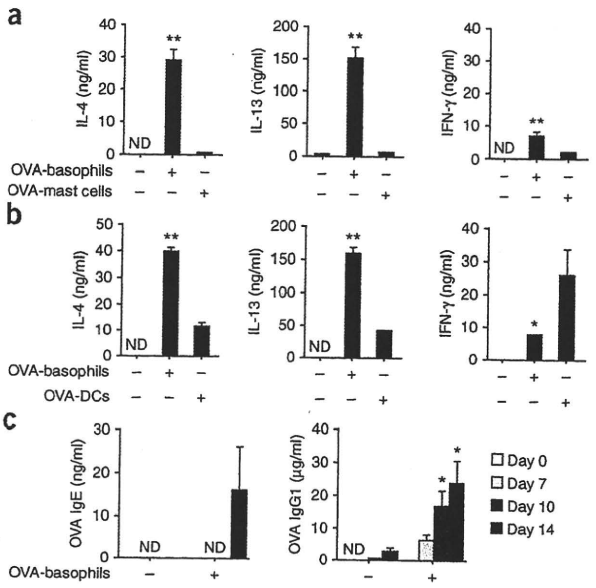

Figure 4 Intravenous administration of OVA-pulsed basophils induces a T_H2 response. (**a**,**b**) Enzyme-linked immunosorbent assay (ELISA) of IL-4, IL-13 and IFN-γ in supernatants of cells prepared as follows: purified bone marrow–derived basophils, mast cells (**a**) or splenic DCs (**b**) stimulated with DNP-OVA plus IgE anti-DNP as described in **Figure 3d** were adoptively transferred into BALB/c mice through the tail vein (2.5×10^5 cells of each per mouse); 4 d later, mice were intravenously challenged with OVA protein (100 μg per mouse) and, 2 d after this challenge, splenic $CD4^+$ T cells from each mouse were restimulated for 5 d in 96-well plates with OVA protein (100 μg/ml) in the presence of irradiated ΔT-spleen cells (1×10^5 cells per 0.2 ml per well for all cells). OVA- (left margin), processed OVA. (**c**) ELISA of OVA-specific IgE and IgG1 in serum from mice treated as follows: after priming of basophils as described in **a**, basophils (5×10^5 cells per mouse) were adoptively transferred into BALB/c mice through the tail vein; 1 week later (day 0), all mice were intravenously challenged with OVA protein (100 μg per mouse) and serum was then collected on days 0–14 (key). *, $P < 0.05$ and **, $P < 0.0001$, OVA-pulsed basophils versus cells from mice given mast cells and injected with OVA protein (**a**), given DCs and injected with OVA protein (**b**) or injected with OVA protein alone (**c**; Student's *t* test). Data are representative of two independent experiments (mean and s.e.m. of five mice).

neutral conditions. Furthermore, basophils had this T_H2-inducing capacity even when the ratio of basophils to $CD4^+$ T cells was decreased to 1:8. As expected, in T_H2 conditions, both types of APCs showed similar APC function. Furthermore, we were able to decrease the ratio of APC to $CD4^+$ T cells to 1:16 without substantially diminishing T_H2 cell development (**Fig. 3e**). In contrast, DCs 'preferentially' induced IFN-γ-producing cells in neutral conditions. Thus, basophils incubated with DNP-OVA and IgE anti-DNP showed very potent OVA-specific T_H2 cell–inducing activity *in vitro*.

OVA-pulsed basophils induce T_H2 cells *in vivo*

We compared the activity of OVA-pulsed basophils and mast cells to induce T_H2 cells *in vivo*. We pulsed basophils and mast cells with OVA by culturing cells with complexes of DNP-OVA and IgE anti-DNP, then transferred these basophils or mast cells into normal mice through the tail vein. Then, 4 d later, we challenged mice intravenously with intact OVA protein in PBS, and 2 d after this challenge, we prepared splenic $CD4^+$ T cells and stimulated them with OVA–pulsed APCs (ΔT-spleen cells) and measured IL-4, IL-13 and IFN-γ in the culture supernatants. We found that only OVA-pulsed basophils promptly and strongly induced T_H2 cells and modestly induced T_H1 cells in the spleen (**Fig. 4a**). We also examined the effect of OVA-pulsed DCs on T_H1 and T_H2 response *in vivo*. Intravenous administration of OVA-pulsed DCs into naive mice dominantly induced T_H1 cells, whereas intravenous administration of OVA-pulsed basophils again induced T_H2 cells strongly and T_H1 cells moderately (**Fig. 4b**), which suggests the importance of basophils in inducing T_H2 responses *in vivo*.

We next examined the ability of mice immunized with OVA-pulsed basophils to produce OVA-specific IgE and IgG1 after OVA challenge. Intravenous administration of OVA solution in naive mice did not induce IgE response but induced a very modest IgG1 response (**Fig. 4c**). In contrast, mice primed with OVA-pulsed basophils produced both IgE and IgG1 in response to OVA (**Fig. 4c**). Indeed, these mice developed $CD4^+CD62L^{lo}IL\text{-}33R\alpha^+$ T_H2 cells in their spleens (**Supplementary Fig. 4a,b** online) that help OVA-activated B cells produce IgE and IgG1 *in vivo*.

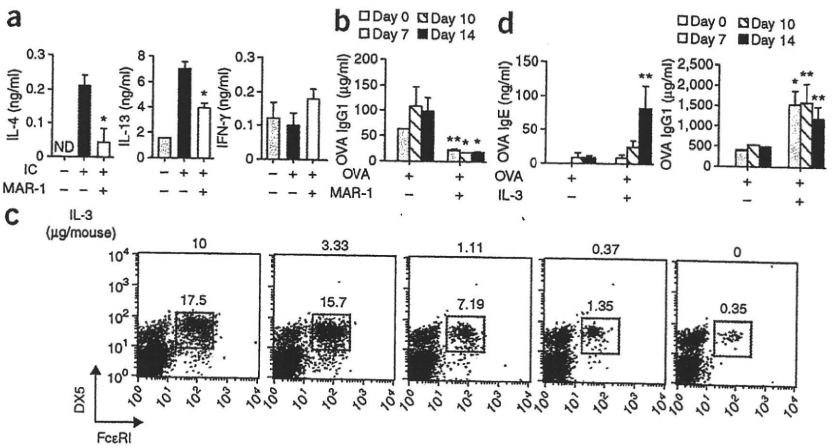

Figure 5 Intravenous administration of antigen-IgE complex induces T_H2 responses. (**a**,**b**) Analysis of cytokines (**a**) and antibodies (**b**) in BALB/c mice pretreated with PBS or anti-FcεRIa (MAR-1) and then injected intravenously with a mixture of DNP-OVA (10 μg) and IgE anti-DNP (20 μg; immune complex (IC)). (**a**) ELISA of IL-4, IL-13 and IFN-γ in supernatants of splenic $CD4^+$ T cells obtained 4 d after injection of the immune complex and restimulated as described in **Figure 4a**. (**b**) OVA-specific IgE and IgG1 antibodies in serum of mice intravenously challenged with OVA protein 4 d after injection of the immune complex, analyzed as described in **Figure 4c**. *, $P < 0.05$ and **, $P < 0.005$, compared with mice given immune complex without MAR-1 pretreatment (Student's *t*-test). (**c**) Frequency of basophils ($FcεRI^+DX5^+$ cells) in BALB/c mice injected with IL-3 (0–10 μg per mouse (above plots) for 2 weeks) via osmotic pump. Numbers above outlined areas indicate percent $FcεRI^+DX5^+$ cells gated on splenic non–B, non–T cells. (**d**) OVA-specific IgE and IgG1 in serum of BALB/c mice pretreated with PBS or IL-3 and then injected intravenously with immune complexes as described in **a**,**b**, then intravenously challenged 4 d later with OVA protein, assessed as described in **Figure 4c**. *, $P < 0.01$ and **, $P < 0.05$, compared with mice without IL-3 pretreatment (Student's *t*-test). Data are representative of two independent experiments (mean and s.e.m. of five mice; **a**,**b**,**d**) or two experiments with five mice (**c**).

Antigen-IgE induces T_H2 cells in a basophil-dependent way

Finally, to demonstrate the contribution of basophils to the development and upregulation of T_H2-IgE response *in vivo*, we intravenously injected complexes of DNP-OVA and IgE anti-DNP into naive mice or mice depleted of basophils by treatment with anti-FcεRIα (MAR-1). As reported by others[38], daily injection of MAR-1 for 3 d almost completely depleted the spleen and liver of basophils (**Supplementary Fig. 5a,b** online). At day 4 after intravenous injection of DNP-OVA (10 μg) and IgE anti-DNP (20 μg), we prepared splenic $CD4^+$ T cells, stimulated them with OVA-pulsed APCs and measured IL-4, IL-13 and IFN-γ in the culture supernatants. We found that IgE immune complexes induced T_H2 cells in the spleens of naive mice (**Fig. 5a**). Depletion of basophils (**Supplementary Fig. 5c,d**) resulted in significantly diminished T_H2 cell development and T_H2-dependent IgG1 responses (**Fig. 5a,b**). These results suggest that basophils efficiently take up DNP-OVA–IgE anti-DNP immune complexes and induce OVA-specific T_H2 cells, which in turn stimulate OVA-stimulated B cells to produce IgG1.

To confirm the contribution of basophils to the initiation and amplification of T_H2-IgE responses, we injected IL-3 into naive mice using an osmotic pump (10 μg IL-3 per 100 μl PBS) to increase the number of basophils and then examined their responsiveness to the treatment with antigen-IgE complex. IL-3-treated mice markedly increased the number of basophils in their spleens (**Fig. 5c**) and other organs, somewhat resembling atopic people, who also increase the number of basophils in inflammation sites[8–11]. We found IL-3-treated mice died of systemic anaphylactic shock when challenged with a high dose of IgE complex (for example, 100 μg DNP-OVA and 200 μg IgE anti-DNP). Therefore, we intravenously injected low doses of IgE complex (5 μg DNP-OVA and 10 μg IgE anti-DNP). In contrast to mice that received no pretreatment with IL-3, IL-3-treated mice significantly increased their production of OVA-specific IgG1 and IgE in response to OVA challenge (**Fig. 5d**), which suggests that the number of basophils might determine the responsiveness to IgE complex that 'preferentially' induces T_H2 cells. These results collectively indicated that basophils are responsible for inducing OVA-specific T_H2 cells by taking up DNP-OVA–IgE anti-DNP complexes, presenting OVA peptide with MHC class II and producing abundant IL-4.

DISCUSSION

Basophils can induce T_H2 cells *in vitro* and *in vivo* by producing early IL-4 (refs. 18,20,29,39). Other studies have shown that basophils that transmigrate to draining lymph nodes after papain stimulation are stimulated to produce IL-4 and/or thymic stromal lymphopoietin, which promote T_H2 differentiation *in vivo*[29]. However, it has remained uncertain whether basophil-derived IL-4 is indeed involved in the development of T_H2 cells in response to stimuli other than protease allergens.

Here we have demonstrated that protein antigen without enzymatic activity induced antigen-specific T_H2 cells *in vitro* and *in vivo* in a basophil- and IL-4-dependent way, which suggests involvement of basophil-derived IL-4 in the development of T_H2 cells. Another important issue that needs to be addressed is the mechanism by which basophils induce T_H2 cells. We could propose at least two mechanisms for basophil-mediated promotion of T_H2 responses. One is that basophils produce IL-4 and/or thymic stromal lymphopoietin and simply transfer foreign protein to DCs, which do the actual antigen presentation. The other is that basophils are APCs that also produce IL-4. We have demonstrated that basophils induce T_H2 cells in the absence of 'professional' APCs *in vitro*. Furthermore, we have shown that basophils are potent APCs that directly and 'preferentially' induce T_H2 cells *in vivo*.

We first demonstrated that basophils derived from mice inoculated with *S. venezuelensis* produced substantial amounts of IL-4, IL-6 and IL-13 in IL-3-containing medium. Then we demonstrated that they expressed MHC class II and strongly induced the development of naive $CD4^+$ T cells into T_H2 cells in neutral conditions. In contrast, basophils from naive mice produced relatively small amounts of IL-4, IL-6 and IL-13 in IL-3-containing medium.

We initially regarded only basophils from infected mice as potent APCs. Then we recognized that basophils from naive mice and infected mice expressed almost identical amounts of MHC class II, which suggested they had a potent APC function. Indeed, splenic basophils in naive mice were also immunologically competent APCs. Both types of basophils produced substantial amounts of IL-10, which suggests the possibility that this IL-10 might enhance the ability of IL-4 from basophils to induce the development of T_H2 cells *in vitro*. Bone marrow basophils also recapitulated well the APC function of splenic basophils. In particular, they were able to efficiently take up a low dose of antigen-IgE complex, present antigen–MHC class II and produce IL-4, which suggests that they are also very potent T_H2 cell–inducing APCs.

We further demonstrated that intravenous administration of OVA-pulsed basophils, which we prepared by culturing basophils with complexes of DNP-OVA and IgE anti-DNP, strongly induced OVA-specific T_H2 cells in the spleens of naive mice. In contrast, OVA-pulsed mast cells failed to do so. These results indicated their difference in inducing antigen-specific T_H2 cells *in vivo*. Basophils have been shown to have a very short half-life after adoptive transfer[40]. Because we cultured basophils with immune complexes of DNP-OVA and IgE anti-DNP, we suspect such crosslinking might induce signals that sustain their survival *in vivo*.

Finally, we demonstrated a single intravenous administration of a low dose of DNP-OVA–IgE anti-DNP complex into naive mice rapidly and 'preferentially' induced OVA-specific T_H2 cells in an endogenous basophil–dependent way. Such sensitized mice then promptly produced antigen-specific IgG1 in response to intravenous administration of antigen solution. As expected, IL-3 treatment prepared mice highly susceptible to the T_H2 cell–inducing action of IgE complex by increasing the number of basophils.

Although basophil MHC class II expression was less than that on conventional APCs, basophils showed more potent T_H2 cell–inducing activity than did conventional APCs in both neutral and T_H2 conditions. We found that basophils had a greater APC activity when pulsed with DNP-OVA in the presence of IgE anti-DNP. We also found that basophils still had the notable T_H2 cell–inducing ability in neutral conditions even when the ratio of APCs to $CD4^+$ T cells was low (1:8). In contrast, OVA-pulsed DCs failed to induce T_H2 cells at any APC/$CD4^+$ T cell ratio in neutral conditions, although they induced IFN-γ-producing cells. Thus, basophils are very potent T_H2 cell–inducing cells *in vitro*.

Our study has indicated that endogenous basophils are important for promotion of the T_H2-IgE response *in vivo*. We demonstrated that intravenous administration of immune complexes of DNP-OVA and IgE anti-DNP 'preferentially' induced OVA-specific T_H2 cells in an endogenous basophil–dependent way. Studies have shown that basophils can also capture antigen by binding to surface antigen-specific IgE-FcεRI (refs. 38,41). Activated basophils then produce IL-4 and IL-6 and possibly express CD40L[42], the ligand for the costimulatory molecule CD40, which in combination induce B cells to proliferate and to produce IgE. Thus, basophils promote both T_H2 and IgE responses *in vivo*.

Atopic people are characterized by having more basophils in sites of allergic inflammation[8–11]. Once atopic people start to produce antigen-specific IgE, they can steadily increase the amount of complexes of

antigen and antigen-specific IgE, which allows basophils to augment their uptake of IgE complex. Although mature human basophils lack HLA-DR, we have shown here that some can re-express HLA-DR when stimulated with IL-3. Thus, it is plausible that mature basophils in the allergic inflammation site, which might be characterized by abundant production of IL-3 and other factors, do express HLA-DR. Basophils, then, could become potent APCs and induce progressive allergic inflammation in these people.

Here we have demonstrated that basophils are important in the amplification of the T_H2-IgE response. Indeed, depletion of basophils by a specific antibody inhibited IgE complex–induced T_H2-IgE responses. Published work has suggested that anti-IgE therapy is effective for T_H2-IgE–mediated diseases[43–45]. The rationale for such therapy is that it is believed to interfere with IgE-mediated activation of mast cells and basophils. On the basis of our results here, we can add another rationale: inhibition of the generation of antigen-pulsed basophils. Thus, basophils might represent an important therapeutic target cell.

METHODS

Methods and any associated references are available in the online version of the paper at http://www.nature.com/natureimmunology/.

Accession codes. UCSD-Nature Signaling Gateway (http://www.signaling-gateway.org): A000543 and A001262.

Note: Supplementary information is available on the Nature Immunology website.

ACKNOWLEDGMENTS

We thank W.E. Paul and H. Yamane for suggestions after critical reading of this manuscript and Y. Taki, H. Seki and S. Futatsugi-Yumikura for technical assistance. Supported by The Japanese Ministry of Education, Culture, Sports, Science and Technology (Grant-in-Aid for Scientific Research on Priority Areas 18073016 and Hitech Research Center Grant), the Japan Society for the Promotion of Science (Grants-in-Aid for Scientific Research 20390145 and 19390121) and the Japanese Ministry of Health, Labor and Welfare (Grants for Research on Emerging and Re-emerging Infectious Diseases).

AUTHOR CONTRIBUTIONS

K.N. and T.Y. envisaged the possible APC function of basophils; T.Y. and K.N. designed the experiments; T.Y. did the main part of this study and analyzed the data; K.Y., M.N. and Y.I. helped with some experimental procedures; H.T. and Y.F. analyzed human cells; and T.Y. prepared the draft of manuscript and K.N. completed it.

Published online at http://www.nature.com/natureimmunology/
Reprints and permissions information is available online at http://npg.nature.com/reprintsandpermissions/

1. Galli, S.J. Mast cells and basophils. *Curr. Opin. Hematol.* **7**, 32–39 (2000).
2. Galli, S.J. *et al.* Mast cells as "tunable" effector and immunoregulatory cells: recent advances. *Annu. Rev. Immunol.* **23**, 749–786 (2005).
3. Kawakami, T. & Galli, S.J. Regulation of mast-cell and basophil function and survival by IgE. *Nat. Rev. Immunol.* **2**, 773–786 (2002).
4. Lantz, C.S. *et al.* IgE regulates mouse basophil FcεRI expression in vivo. *J. Immunol.* **158**, 2517–2521 (1997).
5. Yamaguchi, M. *et al.* IgE enhances mouse mast-cell FcεRI expression in vitro and in vivo: evidence for a novel amplification mechanism in IgE-dependent reactions. *J. Exp. Med.* **185**, 663–672 (1997).
6. Saini, S.S. *et al.* The relationship between serum IgE and surface levels of FcεR on human leukocytes in various diseases: correlation of expression with FcεRI on basophils but not on monocytes or eosinophils. *J. Allergy Clin. Immunol.* **106**, 514–520 (2000).
7. Arinobu, Y. *et al.* Developmental checkpoints of the basophil/mast cell lineages in adult murine hematopoiesis. *Proc. Natl. Acad. Sci. USA* **102**, 18105–18110 (2005).
8. Gauvreau, G.M. *et al.* Increased numbers of both airway basophils and mast cells in sputum after allergen inhalation challenge of atopic asthmatics. *Am. J. Respir. Crit. Care Med.* **161**, 1473–1478 (2000).
9. Irani, A.M. *et al.* Immunohistochemical detection of human basophils in late-phase skin reactions. *J. Allergy Clin. Immunol.* **101**, 354–362 (1998).
10. Koshino, T. *et al.* Airway basophil and mast cell density in patients with bronchial asthma: relationship to bronchial hyperresponsiveness. *J. Asthma* **33**, 89–95 (1996).
11. Macfarlane, A.J. *et al.* Basophils, eosinophils, and mast cells in atopic and nonatopic asthma and in late-phase allergic reactions in the lung and skin. *J. Allergy Clin. Immunol.* **105**, 99–107 (2000).
12. Karasuyama, H., Mukai, K., Tsujimura, Y. & Obata, K. *Nat. Rev. Immunol.* **9**, 9–13 (2009).
13. Mukai, K. *et al.* Basophils play a critical role in the development of IgE-mediated chronic allergic inflammation independently of T cells and mast cells. *Immunity* **23**, 191–202 (2005).
14. Tsujimura, Y. *et al.* Basophils play a pivotal role in immunoglobulin-G-mediated but not immunoglobulin-E-mediated systemic anaphylaxis. *Immunity* **28**, 581–589 (2008).
15. Min, B. Basophils: what they 'can do' versus what they 'actually do'. *Nat. Immunol.* **9**, 1333–1339 (2008).
16. Min, B., Le Gros, G. & Paul, W.E. Basophils: a potential liaison between innate and adaptive immunity. *Allergol. Int.* **55**, 99–104 (2006).
17. Min, B. & Paul, W.E. Basophils and type 2 immunity. *Curr. Opin. Hematol.* **15**, 59–63 (2008).
18. Min, B. *et al.* Basophils produce IL-4 and accumulate in tissues after infection with a Th2-inducing parasite. *J. Exp. Med.* **200**, 507–517 (2004).
19. Sullivan, B.M. & Locksley, R.M. Basophils: a nonredundant contributor to host immunity. *Immunity* **30**, 12–20 (2009).
20. Voehringer, D., Shinkai, K. & Locksley, R.M. Type 2 immunity reflects orchestrated recruitment of cells committed to IL-4 production. *Immunity* **20**, 267–277 (2004).
21. Nakanishi, K., Yoshimoto, T., Tsutsui, H. & Okamura, H. Interleukin-18 is a unique cytokine that stimulates both Th1 and Th2 responses depending on its cytokine milieu. *Cytokine Growth Factor Rev.* **12**, 53–72 (2001).
22. Nakanishi, K., Yoshimoto, T., Tsutsui, H. & Okamura, H. Interleukin-18 regulates both Th1 and Th2 responses. *Annu. Rev. Immunol.* **19**, 423–474 (2001).
23. Takeda, K., Kaisho, T. & Akira, S. Toll-like receptors. *Annu. Rev. Immunol.* **21**, 335–376 (2003).
24. Trinchieri, G. Interleukin-12 and the regulation of innate resistance and adaptive immunity. *Nat. Rev. Immunol.* **3**, 133–146 (2003).
25. Seder, R.A. & Paul, W.E. Acquisition of lymphokine-producing phenotype by $CD4^+$ T cells. *Annu. Rev. Immunol.* **12**, 635–673 (1994).
26. Yoshimoto, T. & Paul, W.E. $CD4^{pos}$, $NK1.1^{pos}$ T cells promptly produce interleukin 4 in response to in vivo challenge with anti-CD3. *J. Exp. Med.* **179**, 1285–1295 (1994).
27. Yoshimoto, T. *et al.* IL-18, although antiallergic when administered with IL-12, stimulates IL-4 and histamine release by basophils. *Proc. Natl. Acad. Sci. USA* **96**, 13962–13966 (1999).
28. Kondo, Y. *et al.* Administration of IL-33 induces airway hyperresponsiveness and goblet cell hyperplasia in the lungs in the absence of adaptive immune system. *Int. Immunol.* **20**, 791–800 (2008).
29. Sokol, C.L., Barton, G.M., Farr, A.G. & Medzhitov, R. A mechanism for the initiation of allergen-induced T helper type 2 responses. *Nat. Immunol.* **9**, 310–318 (2008).
30. Sasaki, Y. *et al.* IL-18 with IL-2 protects against *Strongyloides venezuelensis* infection by activating mucosal mast cell-dependent type 2 innate immunity. *J. Exp. Med.* **202**, 607–616 (2005).
31. Lohning, M. *et al.* T1/ST2 is preferentially expressed on murine Th2 cells, independent of interleukin 4, interleukin 5, and interleukin 10, and important for Th2 effector function. *Proc. Natl. Acad. Sci. USA* **95**, 6930–6935 (1998).
32. Bradley, L.M., Watson, S.R. & Swain, S.L. Entry of naive CD4 T cells into peripheral lymph nodes requires L-selectin. *J. Exp. Med.* **180**, 2401–2406 (1994).
33. Reimer, J.M. *et al.* Isolation of transcriptionally active umbilical cord blood-derived basophils expressing Fc epsilon RI, HLA-DR and CD203c. *Allergy* **61**, 1063–1070 (2006).
34. Hu-Li, J. *et al.* Regulation of expression of IL-4 alleles: analysis using a chimeric GFP/IL-4 gene. *Immunity* **14**, 1–11 (2001).
35. Ben-Sasson, S.Z., Le Gros, G., Conrad, D.H., Finkelman, F.D. & Paul, W.E. Cross-linking Fc receptors stimulate splenic non-B, non-T cells to secrete interleukin 4 and other lymphokines. *Proc. Natl. Acad. Sci. USA* **87**, 1421–1425 (1990).
36. Nakae, S. *et al.* TIM-1 and TIM-3 enhancement of Th2 cytokine production by mast cells. *Blood* **110**, 2565–2568 (2007).
37. Ohteki, T., Suzue, K., Maki, C., Ota, T. & Koyasu, S. Critical role of IL-15-IL-15R for antigen-presenting cell functions in the innate immune response. *Nat. Immunol.* **2**, 1138–1143 (2001).
38. Denzel, A. *et al.* Basophils enhance immunological memory responses. *Nat. Immunol.* **9**, 733–742 (2008).
39. Oh, K., Shen, T., Le Gros, G. & Min, B. Induction of Th2 type immunity in a mouse system reveals a novel immunoregulatory role of basophils. *Blood* **109**, 2921–2927 (2007).
40. Ohnmacht, C. & Voehringer, D. Basophil effector function and homeostasis during helminth infection. *Blood* **113**, 2816–2825 (2008).
41. Mack, M. *et al.* Identification of antigen-capturing cells as basophils. *J. Immunol.* **174**, 735–741 (2005).
42. Gauchat, J.F. *et al.* Induction of human IgE synthesis in B cells by mast cells and basophils. *Nature* **365**, 340–343 (1993).
43. Adcock, I.M., Caramori, G. & Chung, K.F. New targets for drug development in asthma. *Lancet* **372**, 1073–1087 (2008).
44. Okubo, K. & Nagakura, T. Anti-IgE antibody therapy for Japanese cedar pollinosis: omalizumab update. *Allergol. Int.* **57**, 205–209 (2008).
45. Verbruggen, K., Van Cauwenberge, P. & Bachert, C. Anti-IgE for the treatment of allergic rhinitis—and eventually nasal polyps? *Int. Arch. Allergy Immunol.* **148**, 87–98 (2008).

ONLINE METHODS

Mice. BALB/c mice were from Jackson Laboratory. Mice transgenic for αβ TCR recognizing OVA(323–339) (DO11.10) and BALB/c G4-homozygous (IL-4-deficient) mice[34] were bred in specific pathogen–free conditions at the animal facilities of Hyogo College of Medicine. All animal experiments were done in accordance with guidelines of the Institutional Animal Care Committee of Hyogo College of Medicine.

Antibodies and reagents. Anti–mouse IL-4 (11B11)[25] was purified in our laboratory in the Department of Immunology and Medical Zoology, Hyogo College of Medicine. Phycoerythrin (PE)–anti–mouse CD4 (GK1.5), fluorescein isothiocyanate (FITC)–anti–mouse CD62L (MEL-14), FITC–anti–mouse I-A^d (AMS-32.1), FITC–anti–mouse CD40 (HM40-3), FITC–anti–mouse CD80 (16-10A1), FITC–anti–mouse CD86 (GL1), FITC–anti–mouse CD11c (HL3), PE–anti–mouse c-Kit (2BB), FITC–anti–mouse c-Kit (2BB), FITC–anti–mouse CD49b (DX5), FITC–anti–human HLA-DR (TÜ36) and biotin–human CD203c (FR3–16A11) were from BD Biosciences. FITC–anti–mouse ST2 (DJ8), biotin–anti–mouse FcεRIα (MAR-1), streptavidin-PE and streptavidin-allophycocyanin were from eBioscience. The following PE-labeled monoclonal antibodies to human cell surface markers were from BD Biosciences: anti-CD3 (HIT3a), anti-CD7 (M-T701), anti-CD14 (M5E2), anti-CD15 (HI98), anti-CD16 (3G8), anti-CD19 (HIB19), anti-CD36 (CB38), anti-CD45RA (HI100) and anti-CD235a (GAR-2). Recombinant mouse IL-2, IL-3, IL-4 and human IL-3 were from R&D Systems. IL-18 was from MBL. Recombinant human IL-33 was purified in our laboratory in the Department of Immunology and Medical Zoology, Hyogo College of Medicine[28]. Monoclonal IgE anti-DNP (SPE-7), OVA (grade V), lipopolysaccharide from *Salmonella minnesota* Re-595 or *Escherichia coli* 055:B5, and peptidoglycan from *Staphylococcus aureus* were from Sigma. DNP-OVA was prepared according to a published method[46].

Flow cytometry and cell purification. For the preparation of bone marrow–derived basophils, bone marrow cells were cultured for 14 d with IL-3 (10 U/ml) in RPMI-1640 medium supplemented with 10% (vol/vol) FBS, 50 μM 2-mercaptoethanol, 2 mM L-glutamine, 100 U/ml of penicillin and 100 μg/ml of streptomycin (complete RPMI) and were washed twice. Cells were first treated for 30 min at 4 °C with anti–FcγRII/III (10 μg/ml), followed by treatment for 1 h at 4 °C with biotin–anti–mouse FcεRIα (5 μg/ml) in staining buffer (1% (vol/vol) FCS in PBS). After being washed twice, cells were stained for 30 min with streptavidin-allophycocyanin and PE–anti–mouse c-Kit. Samples were analyzed on a FACSCalibur (BD Biosciences) and were separated into $FcεRI^+c\text{-}Kit^-$ cells (basophils) or $FcεRI^+c\text{-}Kit^+$ cells (mast cells) with a FACSAria (BD Biosciences). The purity of each population was over 96%. The resultant populations were further stained with FITC-labeled antibodies for analysis of surface makers. For preparation of splenic basophils, spleen cell samples from BALB/c mice were first depleted of Thy-1.2^+ T cells and $B220^+$ cells with a MACS system (MiltenyiBiotec), then the residual cells were further stained and separated into $FcεRI^+c\text{-}Kit^-$ or $FcεRI^+c\text{-}Kit^+$ cells with a FACSAria. The purity of each population was over 96%. For the preparation of splenic $CD4^+CD62L^+$ resting T cells and for intracellular cytokine staining, published methods were followed[47].

Human peripheral blood from normal volunteers and umbilical cord blood obtained from normal full-term deliveries were obtained and processed after informed consent was given. The Institutional Review Board approved the experimental plan. Mononuclear cells were isolated from peripheral blood and cord blood by Ficoll density-gradient centrifugation. Peripheral blood mononuclear cell samples were further depleted of T cells, monocytes, eosinophils, natural killer cells, B cells, platelets, DCs and erythroid cells magnetically with a 'cocktail' of PE-labeled monoclonal antibodies to human CD3, CD7, CD14, CD15, CD16, CD19, CD36, CD45RA and CD235a and anti-PE MicroBeads (MiltenyiBiotec). Umbilical cord blood mononuclear cells were further enriched to $CD34^+$ cells with MicroBeads. These $CD34^+$ progenitor cells were plated at a density of 5×10^5 cells per ml in 12-well plates and were cultured for 7 d in StemPro-34 SFM (GIBCO) supplemented with 10% (vol/vol) FBS, 50 μM 2-mercaptoethanol, 0.5 mM L-glutamine, 50 U/ml of penicillin, 50 μg/ml of streptomycin and 10 ng/ml of human IL-3.

***In vitro* culture.** Naive splenic $CD4^+CD62L^+$ T cells (1×10^5 cells per ml) from DO11.10 mice were stimulated in 48-well plates with IL-2 (100 pM), IL-3 (20 U/ml) and OVA(323–339) (1 μM) or DNP-OVA (6.25–100 μg/ml) in the presence of conventional APCs (irradiated T cell–depleted BALB/c splenocyte samples), irradiated splenic $CD11c^+$DCs prepared as described[37] or irradiated purified basophils (5×10^5 cells per ml each). For the induction of T_H2 cells, IL-4 (1000 U/ml) was also added to the culture. On the third or fourth day of culture, cells were diluted 1:2 or I:3 in complete RPMI medium with IL-2 (100 pM) and their populations were expanded into 48-well plates. Then, 7 d after the initial stimulation, cells were collected and washed, then were recultured for 4 h with PMA (phorbol 12-myristate 13-acetate; 50 ng/ml) plus ionomycin (500 ng/ml) and were analyzed by flow cytometry for cytosolic IL-4 and IFN-γ. In some experiments, after initial priming, $CD4^+$ T cells (1×10^5 cells per 0.2 ml per well) were restimulated for 48 h in 96-well plates with IL-2 (100 pM) and OVA(323–339) (1 μM) in the presence of 1×10^5 irradiated conventional APCs. Supernatants were collected and cytokine production was assessed with ELISA kits (R&D Systems) or the Bio-Plex system (BioRad) as described before[28].

***In vivo* treatment of mice.** Bone marrow–derived and flow cytometry–sorted basophils, mast cells and splenic $CD11c^+$ DCs (5×10^5 cells per ml each) were cultured for 16 h in 48-well plates with IL-3 (20 U/ml), DNP-OVA (100 μg/ml) and IgE anti-DNP (10 μg/ml). After priming, basophils, mast cells and splenic DCs (2.5×10^5 cells per mouse) were transferred through the tail vein into BALB/c mice. At 4 d or 1 week after reconstitution, mice were intravenously challenged with OVA protein (100 μg) in PBS. In some experiments, BALB/c mice were injected intravenously with a mixture of DNP-OVA (5–100 μg per mouse) and IgE anti-DNP (10–200 μg per mouse). For *in vivo* depletion of basophils, a published method of was followed[38]. Mice were injected intraperitoneally twice daily for 3 d with 5 μg anti–mouse FcεRIα (MAR-1) or PBS. Mice were allowed to 'rest' for 2 d and then were injected with a mixture of DNP-OVA plus IgE anti-DNP, then these mice were injected twice daily for additional 3 d with MAR-1 or PBS. IL-3 was infused subcutaneously into mice via osmotic pumps (Durect) filled with IL-3 (100 μg) in 100 μl PBS in mice as described[48].

ELISA. OVA-specific serum IgE was measured with a Mouse OVA-IgE ELISA kit (Dainippon Sumitomo Pharma). OVA-specific serum IgG1 was measured with a Mouse OVA-IgG1 ELISA kit (AKRIE-04; Shibayagi).

Parasites. BALB/c mice were subcutaneously inoculated with 5,000 *S. venezuelensis* third-stage larvae to initiate complete infection as described[27,30].

Electron microscopy. Sorted human $CD203c^+HLA\text{-}DR^+$ cells were fixed with 2% (wt/vol) paraformaldehyde and 1.25% (wt/vol) glutaraldehyde, were post-fixed with 1% (wt/vol) OsO_4 and were embedded in Epon. Ultrathin sections were double-stained with uranyl acetate and lead citrate and were examined with a JEM 1220 transmission electron microscopy (Jeol).

Proliferation assay. Naive splenic $CD4^+CD62L^+$ T cells from DO11.10 mice (5×10^4 cells per 0.2 ml per well) were stimulated for 4 d in 96-well plates with IL-2 (100 pM), IL-3 (20 U/ml) and OVA(323–339) (1 μM) or DNP-OVA (6.25–100 μg/ml) with or without monoclonal anti-DNP IgE (10 μg/ml) in the presence of conventional APCs or purified basophils (2.5×10^5 cells per well each). DNA synthesis was assessed by measurement of the incorporation of 0.2 μCi [^{3}H]thymidine during the final 16 h.

Analysis of expression of TLR mRNA. Total RNA was extracted from sorted basophils and mast cells with TRIzol reagent, was treated with DNase I and was reverse-transcribed with SuperScript II Reverse Transcriptase and oligo$(dT)_{12–18}$ primer (Invitrogen). As a positive control for each TLR, RNA extracted from total spleen cells was used. For analysis of expression of TLR mRNA, mRNA was amplified by a modified standard RT-PCR amplification procedure. The specific TLR primer sequences and their annealing

doi:10.1038/ni.1737

temperatures were according to a published report[49]. PCR conditions were as follows: cDNA was amplified by 35 cycles of 95 °C for 30 s, 55 °C for 30 s and 72 °C for 30 s, followed by further extension at 72 °C for 10 min, then samples were stored at 4 °C until analysis. After amplification, PCR products were separated by electrophoresis through 1.7% agarose gels and were visualized by illumination with ultraviolet light.

Statistics. Statistical comparisons between two experimental groups were made with a paired Student's *t*-test using GraphPad Instat Software. *P* values of less than 0.05 were considered significant.

46. Eisen, H.N., Carsten, M.E. & Belman, S. Studies of hypersensitivity to low molecular weight substances. III. The 2,4-dinitrophenyl group as a determinant in the preciptin reaction. *J. Immunol.* **73**, 296–308 (1954).
47. Yoshimoto, T., Yoshimoto, T., Yasuda, K., Mizuguchi, J. & Nakanishi, K. IL-27 suppresses Th2 cell development and Th2 cytokines production from polarized Th2 cells: a novel therapeutic way for Th2-mediated allergic inflammation. *J. Immunol.* **179**, 4415–4423 (2007).
48. Kosaka, H., Yoshimoto, T., Yoshimoto, T., Fujimoto, J. & Nakanishi, K. Interferon-gamma is a therapeutic target molecule for prevention of postoperative adhesion formation. *Nat. Med.* **14**, 437–441 (2008).
49. Caramalho, I. *et al.* Regulatory T cells selectively express toll-like receptors and are activated by lipopolysaccharide. *J. Exp. Med.* **197**, 403–411 (2003).

doi:10.1038/ni.1737

ESTABLISHMENT OF A CONTINUOUS CULTURE SYSTEM FOR *ENTAMOEBA MURIS* AND ANALYSIS OF THE SMALL SUBUNIT rRNA GENE

KOBAYASHI S.*, SUZUKI J.** & TAKEUCHI T.*

Summary:

We established a culture system for *Entamoeba muris* (MG-EM-01 strain isolated from a Mongolian gerbil) using a modified Balamuth's egg yolk infusion medium supplemented with 4 % adult bovine serum and *Bacteroides fragilis* cocultured with *Escherichia coli*. Further, encystation was observed in the culture medium. The morphological characteristics of *E. muris* are similar to those of *Entamoeba coli* (*E. coli*); moreover, the malic isoenzyme electrophoretic band, which shows species-specific electrophoretic mobility, of *E. muris* had almost the same mobility as that observed with the malic isoenzyme electrophorectic band of *E. coli* (UZG-EC-01 strain isolated from a gorilla). We determined the small subunit rRNA (SSU-rRNA) gene sequence of the MG-EM-01 strain, and this sequence was observed to show 82.7 % homology with that of the UZG-EC-01 strain. Further, the resultant phylogenetic tree for molecular taxonomy based on the SSU-rRNA genes of the 21 strains of the intestinal parasitic amoeba species indicated that the MG-EM-01 strain was most closely related to *E. coli*.

KEY WORDS : *Entamoeba muris, Entamoeba coli,* dixenic culture, Balamuth's egg yolk infusion medium, SSU-rRNA gene, phylogenetic analysis.

Résumé : ÉTABLISSEMENT D'UN SYSTEME DE CULTURE SUCCESSIVE POUR *ENTAMOEBA MURIS* ET ANALYSE DU GÈNE CODANT POUR LA PETITE SOUS-UNITÉ DE L'ARNr

*Un système de culture d'*Entamoeba muris *(souche MG-EM-01, isolée da la gerbille de Mongolie) a été établi en utilisant un milieu d'infusion de vitellus de Balamuth modifié, supplémenté avec 4 % de sérum bovin adulte et de* Bacteroides fragilis *en coculture avec* Eschericia coli. *L'enkystement s'est également présenté dans le milieu de culture. Les aspects morphologiques d'*E. muris *sont semblables à ceux d'*Entamoeba coli *et la bande isoenzymatique malique présentant une mobilité électrophorétique spécifique à l'espèce avait à peu près la mobilité d'*Entamoeba coli *(souche UZG-EC-01, isolée d'un gorille). La séquence du gène codant pour la petite sous-unité de l'ARNr (SSU-rRNA) de la souche MG-EM-01 a été déterminée et l'homologie de la séquence était également identique à 82,7 % de celle de la souche UZG-EC-01. L'arbre phylogénétique qui en résulte pour la taxonomie moléculaire basée sur les gènes SSU-rRNA de 21 souches d'espèces de parasites intestinaux amibiens indiquait également que la souche MG-EM-01 était étroitement liée à* E. coli.

MOTS CLÉS : Entamoeba muris, Entamoeba coli, *culture dixenic, milieu d'infusion de vitellus de Balamuth, petite sous-unité de l'ARNr, analyse phylogénétique.*

Entamoeba muris is a highly contagious intestinal protozoan parasite of laboratory mice, rats and other rodents; this species is morphologically similar to *Entamoeba coli* (*E. coli*) (Neal, 1950) and primarily proliferates and encysts in the caecum of mice (Lin, 1971).

In vitro culture of *E. muris* has been attempted (Neal, 1950; Simitch & Petrovitch, 1951; Smith *et al.*, 1985); however, trials to achieve successive culture have not been successful.

In the present study, we established a system for the stable and successive culture of an *E. muris* strain. Further, we attempted phylogenetic analysis of this strain to help in investigating its molecular taxonomy.

MATERIALS AND METHODS

E. muris (strain MG-EM-01) isolated from a Mongolian gerbil spontaneously infected in our laboratory was used to establish the culture system. An *E. coli* strain (UZG-EC-01) isolated from a gorilla in a zoo in Tokyo, Japan, was used as a reference. *Escherichia coli* and *Bacteroides fragilis* strains were isolated from the stool of a primate [DeBrazza's guenon (*Cercopithecus neglectus*)] and fresh human stool samples from a patient with intestinal amoebic colitis, respectively. The *E. coli* strains were maintained in a chemically defined medium (R medium) (Robinson, 1968), and the *B. fragilis* strains were maintained on trypticase, yeast extract and iron (TYI) broth (Diamond *et al.*, 1978); these strains were used as supplements for the culture system of *E. muris*.

* Department of Tropical Medicine and Parasitology, School of Medicine, Keio University, Tokyo, Japan.
** Division of Clinical Microbiology, Department of Microbiology, Tokyo Metropolitan Institute of Public Health, Tokyo, Japan.
Correspondence: Seiki Kobayashi, Ph.D., Department of Tropical Medicine and Parasitology, School of Medicine, Keio University, Shinjuku-ku, Tokyo 160-8582, Japan.
Tel: +81 3 5363 3761 – Fax: +81 3 3353 5958.
E-mail: skobaya@sc.itc.keio.ac.jp

The egg yolk infusion medium of Balamuth's medium (Balamuth, 1946) was replaced with infusion of a liver concentrate with 4 % preheat-treated adult bovine serum (56° C for three hours). At least one day prior to *E. muris* culture, 0.1 ml of *E. coli* maintained in the R suspension was added from the stock culture preserved at 4° C (used within one month); however, 0.2 ml of a 1- to 3-day culture of *B. fragilis* maintained in TYI broth was added to the abovementioned culture at the time of *E. muris* primary culture. The primary culture of *E. muris* was performed by inoculating cysts obtained from the stool sample of a Mongolian gerbil; this inoculation was performed after killing the concomitant enteric bacteria with 0.1 N HCl for 60 min at 35.5° C, and subsequent inoculation with a newly designed excystation medium (0.25 % trypsin, 0.24 % gall powder, and lipase (840 units/ml) from *Chromobacterium viscosum* (Sigma-Aldrich Corp., St. Louis, MO, USA) in Hanks' balanced salt solution) for 60 min at 35.5° C.

For 120 hours, the number of trophozoites in 5 µl of the abovementioned culture was counted microscopically at 24-hours intervals, as described previously (Kobayashi *et al.*, 2005). The resistance of the cysts to osmotic pressure was confirmed using 0.05 % sarcosyl (Eichinger, 1997) over a 24-hours period. The viability of the cysts was assessed by double-fluorescence staining using acridine orange and ethidium bromide (Parks *et al.*, 1979). The number of cysts in 5 µl of the homologous amoeba suspension in 0.05 % sarcosyl, which was adjusted to the same volume as that of the culture medium, was counted microscopically in a manner similar to that described previously (Kobayashi *et al.*, 2005).

In order to characterize the trophozoites, we performed isoenzyme analyses (zymodeme) (Sargeaunt, 1988) of *E. muris* and *E. coli.*

The primers for amplification of the SSU-rRNA gene sequences of the *E. muris* (MG-EM-01) and *E. coli* (UZG-EC-01) isolates were designed on the basis of the two SSU-rRNA sequences of *E. coli* [IH:96/135 (AF149914) and HU-1:CDC (AF149915)] acquired from GenBank. Table I lists the three primer sets designed, namely, Ecoli1F/Ecoli1R, Ecoli2F/Ecoli2R and Ecoli3F/Ecoli3R. The polymerase chain reaction (PCR) amplification and the sequencing analysis of the PCR products of the SSU-rRNA genes derived from MG-EM-01 and UZG-EC-01 were performed as described previously (Suzuki *et al.*, 2008).

Analysis and multiple alignments of the acquired sequences of the SSU-rRNA genes of *E. muris* (MG-EM-01) and *E. coli* (UZG-EC-01) were performed by following the Yebis system for DNA Alignment, which uses a tree-based round-robin iterative algorithm (Hirosawa *et al.*, 1995). The phylogenetic tree was constructed using PhyML software package version 2.4.5 (Guindon and Gascuel, 2003) using maximum likelihood (ML) analysis and a general time-reversible (GTR) model to calculate genetic distances. The reliability of the branches of the tree of the GTR model was tested with bootstrap values obtained from 1,000 replications. The ML tree data file from PhyML was read, and the tree was constructed using MEGA software (Tamura *et al.*, 2007).

RESULTS

We have been successfully culturing *E. muris* for greater than 16 months now. Fig. 1 shows the growth and encystation kinetics of *E. muris* maintained in modified Balamuth's medium. Encystation of *E. coli* isolates was not observed in this medium. The mean sizes of trophozoites (33.3 ± 8.9 × 21.6 ± 5.6 µm) and cysts (21.6 ± 3.0 × 20.8 ± 2.3 µm) of *E. muris* in the culture medium were almost the same as those of *E. coli* trophozoites (32.8 ± 12.6 × 28.4 ± 7.6 µm) and cysts (21.6 ± 6.1 × 19.8 ± 3.8 µm). However, similar to the result reported by Neal (1950), a greater number of trophozoites and cyst nuclei with extremely eccentric karyosomes and thin peripheral chromatin layers were observed in *E. muris* compared to *E. coli.* Additionally, a large chromatin mass in the polar position of the karyosome in the nucleus of the *E. muris* cyst was frequently observed in the cysts reproduced in the *in vitro* culture (Fig. 2).

Figure 3 shows a representation of the zymodeme analyses to estimate malic enzyme (ME) and hexokinase (HK) levels. The electrophoretic mobility of the single band of *E. muris* ME was almost the same as that observed with *E. coli* ME. However, the electrophoretic

Primer name	Primer sequence (5' to 3')	Nucleotide position*
Ecoli1F (forward)	GTT GAT CCT GCC AGT ATT ATA TG	7-28
Ecoli1R (reverse)	ATA CCA TGC TTC ATC ATT C	841-859
Ecoli2F (forward)	GTA ATT CCA GCT CCA ATA GTC	617-637
Ecoli2R (reverse)	AAG TTC AAG TCT CGT TCG TTA TCG GA	1467-1492
Ecoli3F (forward)	TGA CTC AAC ACG GGA AAA CTT	1339-1359
Ecoli3R (reverse)	ATC CTT CCG CAG GTT CAC CTA C	2083-2104

* Nucleotide position was based on sequence of *Entamoeba coli* UZG-EC-01 Srain (AB444953).

Table I. – Oligonucleotide primers used for PCR assays in present study.

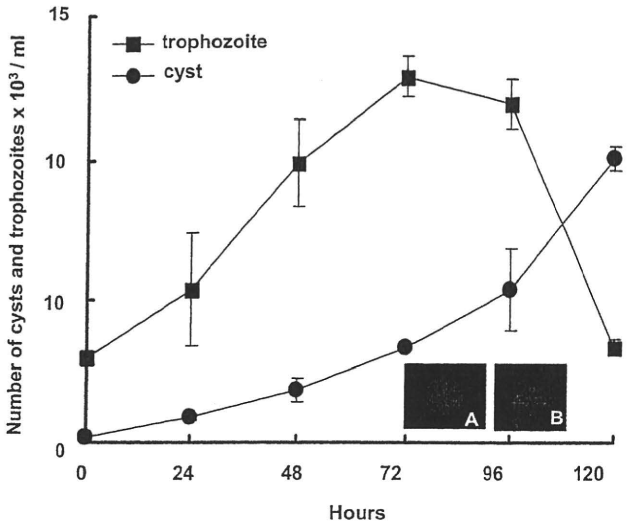

Fig. 1. – Growth kinetics of *Entamoeba muris* strain MG-EM-01 with reproduction of cysts in newly modified Balamuth's medium. The mean number of trophozoites and cysts in duplicate cultures are plotted. A and B, micrographs of cysts that were double-fluorochrome stained with acridine orange (AO) and ethidium bromide (EB). Live cysts (A) are stained with only AO (green colour); however, dead cysts (B) are stained with both AO and EB (red colour).

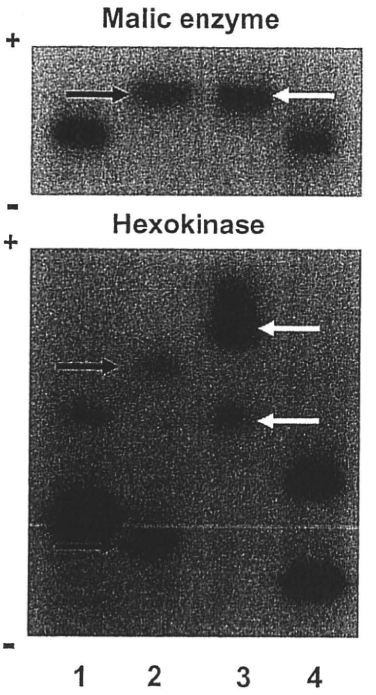

Fig. 3. – Isoenzyme pattern of malic enzyme and hexokinase of four strains of four different *Entamoeba* species. Lane 1, HM-1:IMSS clone 6 (*Entamoeba histolytica*); Lane 2, MG-EM-01 (*Entamoeba muris*); Lane 3, UZG-EC-01 (*Entamoeba coli*); Lane 4, AS 16 IR (*Entamoeba dispar*).

mobility of the double bands of *E. muris* HK showed a pattern that was different from that observed with *E. coli* HK, HM-1:IMSS clone 6 (ATCC 50527) (*E. histolytica*) HK, and AS 16 IR (*E. dispar*) HK (Kobayashi *et al.*, 2005) (Fig. 3). Under these electrophoretic conditions, distinguishable bands of phosphoglucomutase (PGM) and glucose phosphate isomerase (GPI) were observed neither in *E. muris* nor in *E. coli*.

On the basis of phylogenetic analysis, these four strains of *E. coli* and *E. muris* were included in the genus *Entamoeba* and the eight nuclei per cyst group were sister taxa in 100 % of the bootstrap resamplings (Fig. 4).

DISCUSSION

Escherichia coli, a facultative anaerobic bacterium, can produce anaerobic conditions that facilitate the culture of certain obligate anaerobic bacteria such as *B. fragilis*; this principle has been used in a coculture system with *Escherichia coli* in Robin-

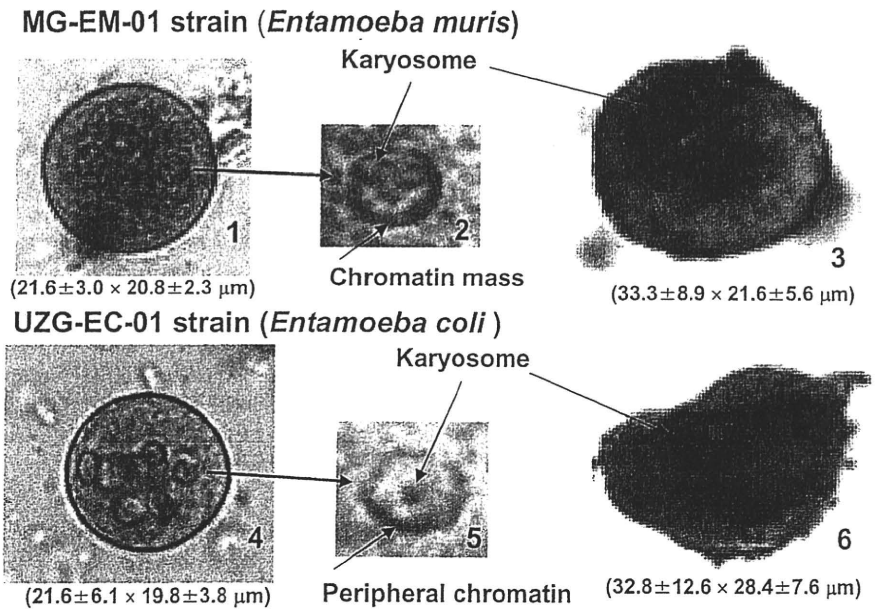

Fig. 2. – Micrographs of cysts and trophozoites of *Entamoeba muris* strain MG-EM-01 and *Entamoeba coli* strain UZG-EC-01. 1 and 4, cysts of MG-EM-01 (1) and UZG-EC-01 (4) strains stained with Lugol's iodine solution (Lugol). 2 and 5, nuclei of MG-EM-01 (2) and UZG-EC-01 (5) strains stained with Lugol. 3 and 6, trophozoites of MG-EM-01 (3) and UZG-EC-01 (6) strains stained with Kohn's chlorazol black E (Gleason *et al.*, 1965).

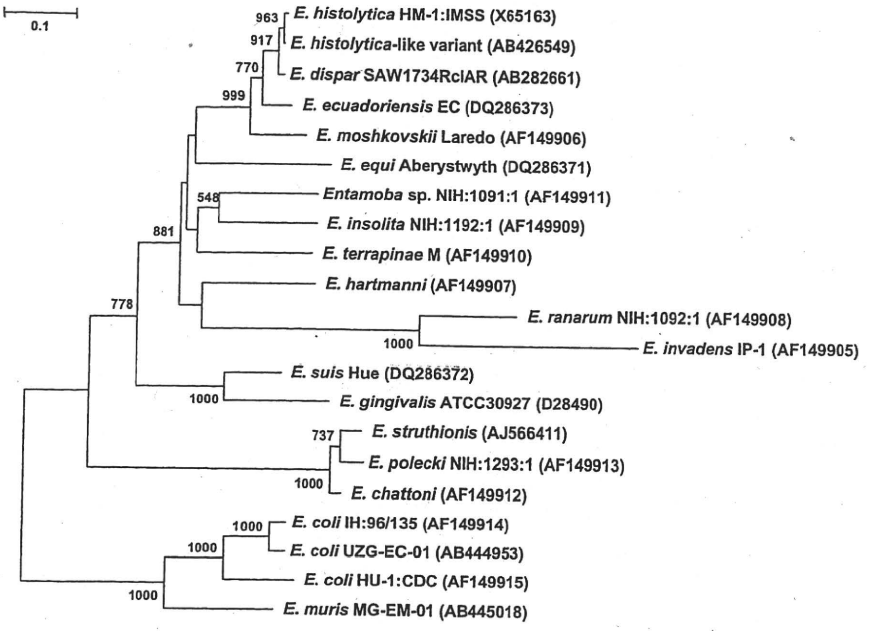

Fig. 4.— An unrooted phylogenetic reconstruction based on the SSU-rRNA gene sequences that explores the relationships among *Entamoeba* species is shown. A maximum likelihood (ML) tree derived using a general time reversible (GTR) model employing estimates of the proportion of invariable sites and the gamma distribution parameter of 0.423 and 0.169, respectively. Significant bootstrap support (> 500) from 1,000 replicates is indicated on the left of the supported node. The scale bar represents the evolutionary distance for the number of changes per site. The numbers within parentheses represent the corresponding GenBank accession numbers.

son's medium (Robinson, 1968). Some obligate anaerobic bacteria such as *Fusobacterium symbiosum* (*Clostridium symbiosum* ATCC 14940) (Diamond, 1983) can promote the growth of human parasitic *Entamoeba* isolates. Therefore, an isolate of *B. fragilis* that demonstrated a growth-promoting effect on the wild isolates of *E. histolytica* and *E. coli* in Balamuth's egg yolk infusion medium (data not shown) was used as a supplement for the culture of *E. muris;* thereafter, a successful culture system for *E. muris* was established for the first time. Phylogenetic analysis of the SSU-rRNA gene sequence of the *E. muris* (MG-EM-01) isolates, although derived from only one strain, suggested that *E. muris* is phylogenetically similar to *E.coli* that produced cysts with eight nuclei. The correlation between phylogenetic propinquity and the number of nuclei observed in the *Entamoeba* species possessing four nuclei per cyst has been previously reported (Silberman *et al.*, 1999; Clark *et al.*, 2006).
The established culture system continues to be dixenic. However, it enabled the analysis of the biological and molecular characteristics of an *E. muris* strain.

ACKNOWLEDGEMENTS

This work was supported by a Health Sciences Research Grant-in-Aid (Research project No. 016) for Emerging and Reemerging Infectious Diseases and the Keio Gijuku Fukuzawa Memorial Fund for the Advancement of Education and Research.

REFERENCES

BALAMUTH W. Improved egg yolk infusion for cultivation of *Entamoeba histolytica* and other intestinal protozoa. *American Journal of Clinical Pathology*, 1946, *16*, 380-384.

CLARK C.G., KAFFASHIAN F., TAWARI B., WINDSOR J.J., TWIGG-FLESNER A., DAVIES-MOREL M.C., BLESSMANN J., EBERT F., PESCHEL B., LE VAN A., JACKSON C.J., MACFARLANE L. & TANNICH E. New insights into the phylogeny of *Entamoeba* species provided by analysis of four new small-subunit rRNA genes. *International Journal of Systematic and Evolutionary Microbiology*, 2006, *56*, 2235-2239.

DIAMOND L.S., HARLOW D.R. & CUNNICK C.C. A new medium for the axenic cultivation of *Entamoeba histolytica* and other *Entamoeba*. *Transactions of the Royal Society of Tropical Medicine and Hygiene*, 1978, *72*, 431-432.

DIAMOND L.S. Lumen-dwelling protozoa: *Entamoeba*, trichomonads and *Giardia*, *in*: *In vitro* cultivation of Protozoan parasites. Jensen J.B. (ed.), CRC press, Boca Raton, Florida, 1983, 65-109.

EICHINGER D. Encystation of *Entamoeba* parasites. *BioEssays*, 1997, *19*, 633-639.

GLEASON N.N. & HEALY G.R. Modification and evaluation of Kohn's one-step staining technique for intestinal protozoa in feces or tissue. *Technical Bulletin of the Registry of Medical Technologists*, 1965, *35*, 64-66.

GUINDON S. & GASCUEL O. A simple, fast, and accurate algorithm to estimate large phylogenies by maximum likelihood. *Systematic Biology*, 2003, *52*, 696-704.

HIROSAWA M., TOTOKI Y., HOSHIDA M. & ISHIKAWA M. Comprehensive study on iterative algorithms of multiple sequence alignment. *Computer Applications in the Biosciences*, 1995, *11*, 13-18.

KOBAYASHI S., IMAI E., HAGHIGHI A., KHALIFA S.A.M., TACHIBANA H. & TAKEUCHI T. Axenic cultivation of *Entamoeba dispar* in newly designed yeast extract-iron-gluconic acid-dihydroxyacetone-serum medium. *Journal of Parasitology*, 2005, *91*, 1-4.

LIN T.M. Colonization and encystation of *Entamoeba muris* in the rat and the mouse. *Journal of Parasitology*, 1971, *57*, 375-382.

NEAL R.A. An experimental study of *Entamoeba muris* (Grassi, 1879); its morphology, affinities and host-parasite relationship. *Parasitology,* 1950, *40*, 343-365.

PARKS D.R., BRYAN V.M., OI V.T. & HERZENBERG L.A. Antigen-specific identification and cloning of hybridomas with a fluorescence-activated cell sorter. *Proceedings of the National Academy of Sciences of the United States of America,* 1979, *76*, 1962-1966.

ROBINSON G.L. Laboratory cultivation of some human parasitic amoebae. *Journal of General Microbiology,* 1968, *53*, 69-79.

SARGEAUNT P.G. Zymodemes of *Entamoeba histolytica, in:* Amebiasis: human infection by *Entamoeba histolytica.* Radvin J.I. (ed.), John Wiley and Sons, Inc., New York, 1988, 370-387.

SILBERMAN J.D., CLARK C.G., DIAMOND L.S. & SOGIN M.L. Phylogeny of the genera *Entamoeba* and *Endolimax* as deduced from small-subunit ribosomal RNA sequences. *Molecular Biology and Evolution,* 1999, *16*, 1740-1751.

SIMITCH T. & PETROVITCH Z. Culture of *Entamoeba muris* of the mouse at the temperature of 22-23° C. *Annales de Parasitologie Humaine et Comparée,* 1951, *26*, 389-393.

SMITH J.M., CHADEE K. & MEEROVITCH E. Failure to establish experimental *Entamoeba histolytica* infection in Mongolian gerbils (*Meriones unguiculatus*) naturally infected with *Entamoeba muris. Transactions of Royal Society of Tropical Medicine and Hygiene,* 1985, *79*, 875-876.

SUZUKI J., KOBAYASHI S., MURATA R., TAJIMA H., HASHIZAKI F., YANAGAWA Y. & TAKEUCHI T. A survey of amoebic infections and differentiation of an *Entamoeba histolytica*- like variant (JSK2004) in nonhuman primates by a multiplex polymerase chain reaction. *Journal of Zoo and Wildlife Medicine,* 2008, *39*, 370-379.

TAMURA K., DUDLEY J., NEI M. & KUMAR S. Molecular evolutionary genetics analysis (MEGA) software version 4.0. *Molecular Biology and Evolution,* 2007, *24*, 1596-1599.

Reçu le 12 novembre 2008
Accepté le 3 février 2009

G Model
ANTAGE-3125; No. of Pages 6
ARTICLE IN PRESS

International Journal of Antimicrobial Agents xxx (2009) xxx–xxx

Contents lists available at ScienceDirect

International Journal of Antimicrobial Agents

journal homepage: http://www.elsevier.com/locate/ijantimicag

Cytotoxic effect of amide derivatives of trifluoromethionine against the enteric protozoan parasite *Entamoeba histolytica*

Dan Sato[a,b], Seiki Kobayashi[c], Hiroyuki Yasui[d], Norio Shibata[d], Takeshi Toru[d], Masaichi Yamamoto[e], Gensuke Tokoro[e], Vahab Ali[f,1], Tomoyoshi Soga[a], Tsutomu Takeuchi[c], Makoto Suematsu[b], Tomoyoshi Nozaki[f,g,*]

[a] *Institute for Advanced Biosciences, Keio University, Tsuruoka, Yamagata 997-0052, Japan*
[b] *Center for Integrated Medical Research, School of Medicine, Keio University, Shinjuku, Tokyo 160-8582, Japan*
[c] *Department of Parasitology, School of Medicine, Keio University, Shinjuku, Tokyo 160-8582, Japan*
[d] *Department of Frontier Materials, Graduate School of Engineering, Nagare College, Nagoya Institute of Technology, Nagoya 466-8555, Japan*
[e] *aRigen Pharmaceuticals Incorporated, 7-3-37/3F, Akasaka, Minato-ku, Tokyo 107-0052, Japan*
[f] *Department of Parasitology, Gunma University Graduate School of Medicine, Maebashi, Gunma, Japan*
[g] *Department of Parasitology, National Institute of Infectious Diseases, Shinjuku, Tokyo 162-8640, Japan*

ARTICLE INFO

Article history:
Received 23 April 2009
Accepted 3 August 2009

Keywords:
Drug discovery
Sulphur-containing amino acid metabolism
Methionine γ-lyase
Protozoan parasite

ABSTRACT

Amoebiasis, caused by infection with the enteric protist *Entamoeba histolytica*, is one of the major parasitic diseases. Although metronidazole and its derivatives are currently employed in therapy, the paucity of effective drugs and potential clinical resistance necessitate the development of a novel drug. Trifluoromethionine (TFM) is a promising lead compound for antiamoebic drugs. To potentiate the antiamoebic effect of TFM, we synthesised various amide derivatives of TFM and evaluated their cytotoxicity. The amide derivatives of TFM were observed to have a superior cytotoxic effect compared with TFM and metronidazole against *E. histolytica* in vitro. Although TFM showed cytotoxicity following degradation by methionine γ-lyase, the derivatives were degraded by the enzyme less efficiently compared with TFM. We further demonstrated that a representative derivative was hydrolysed by the amoebic cell lysate to first yield TFM, followed by degradation similar to TFM. Hydrolysis was partially inhibited by protease inhibitors. A single subcutaneous or oral administration of TFM and its amide derivatives also effectively prevented the formation of amoebic liver abscess in a rodent model. These data demonstrate the improved effectiveness of TFM derivatives against *E. histolytica* infection and elucidate the mechanisms underlining the mode of action of these compounds.

1. Introduction

Amoebiasis is an infectious disease caused by the enteric protozoan parasite *Entamoeba histolytica* and is the second leading cause of death from parasitic diseases after malaria. Only metronidazole and related compounds are commonly used against invasive intestinal and extraintestinal amoebiasis [1,2]. Although clinical resistance against metronidazole has not yet been demonstrated, sporadic cases of treatment failure have been reported [1]. In addition, it has been shown that this parasite easily adapts to therapeutic levels of metronidazole in vitro [3]. Resistance to metronidazole is also acquired easily by many bacterial species as well as *Giardia intestinalis* and *Trichomonas vaginalis* [1]. Therefore, the development of a novel antiamoebic drug is urgently required.

Pathways present exclusively in microorganisms but missing in humans may potentially represent a rational target for drug development. *Entamoeba histolytica* has several unique metabolic features. It lacks both the forward and reverse trans-sulphuration pathways that convert methionine to cysteine via cystathionine or vice versa, whilst it possesses L-methionine γ-lyase (MGL) (EC. 4.4.1.11) to decompose methionine, homocysteine and cysteine and produces ammonia, α-keto acid and volatile thiols [4]. MGL is present in only limited lineages of bacteria, parasitic protozoa and plants but is absent in mammals (see in [5]). In *E. histolytica*, two isoenzymes of MGL (MGL1 and MGL2) with distinct substrate specificities have been identified [5].

Trifluoromethioninė (TFM), also know as *S*-trifluoromethyl-L-homocysteine, a fluorinated analogue of methionine, has been

* Corresponding author. Present address: Department of Parasitology, National Institute of Infectious Diseases, 1-23-1 Toyama, Shinjuku, Tokyo 162-8640, Japan. Tel.: +81 3 5285 1111x2600; fax: +81 3 5285 1219.
E-mail address: nozaki@nih.go.jp (T. Nozaki).
[1] Present address: Department of Biochemistry, Rajendra Memorial Research Institute of Medical Sciences, Agam Kuan, Patna 800007, India.

0924-8579/$ – see front matter © 2009 Elsevier B.V. and the International Society of Chemotherapy. All rights reserved.
doi:10.1016/j.ijantimicag.2009.08.016

shown to be highly toxic to bacteria, *Porphyromonas gingivalis*, *T. vaginalis* and *E. histolytica* in vitro [6–9]. It was also reported to treat infections by *P. gingivalis* and *T. vaginalis* in a rodent model [7,8]. In the present study, the in vitro and in vivo efficacy of TFM and its derivatives were examined to gain insight into the structure–activity relationship and to determine the mechanism underlying their mode of action.

2. Materials and methods

2.1. Chemical synthesis of trifluoromethionine and its derivatives

The synthetic scheme and structure of TFM and its analogues are shown in Supplementary Fig. 1.

2.2. Parasites and cultivation

Trophozoites of *E. histolytica* HM-1:IMSS cl6 were cultured axenically in BIS medium at 35.5 °C as described previously [10].

2.3. In vitro cytotoxicity assay of trifluoromethionine derivatives against Entamoeba histolytica trophozoites and Chinese hamster ovary (CHO) cells

Approximately 5×10^3 amoebae in 280 μL of medium were seeded into each well of a 96-well plate and incubated with various concentrations of TFM derivatives for 48 h. Following incubation, the amoebae were washed with 100 μL of pre-warmed Opti-MEM® I (Invitrogen, Carlsbad, CA) and viable cells were counted using Cell Proliferation Reagent WST-1 (Roche Diagnostics, Mannheim, Germany). Cytotoxicity against mammalian cells was examined as described above except that 1×10^4 CHO cells were cultivated in 280 μL of F-12 medium (Invitrogen) under 5% CO_2 at 37 °C.

2.4. Assay for L-methionine γ-lyase activity

Recombinant MGL1 (3 μg) or MGL2 (1.2 μg) (final concentrations 15 μg/mL and 6 μg/mL, respectively) [5] was incubated with 1 mM TFM, anilide (TFM-01) or benzylamide (TFM-02) in 200 μL of 100 mM sodium phosphate buffer (pH 7.2) containing 20 μM pyridoxal-5′-phosphate (PLP) and 2.5 mM 5,5′-dithiobis(2-nitrobenzoic acid) (Sigma, St Louis, MO) at 37 °C. Released thiols were measured as described previously [9].

2.5. Degradation of trifluoromethionine derivatives in amoebic cell lysate determined by capillary electrophoresis with electrospray ionisation time-of-flight mass spectrometry (CE-TOFMS)

Approximately 3×10^6 trophozoites were lysed with 450 μL of 10 mM HEPES (pH 7.5) containing 1 μM PLP and 0.05% Tween 20. The filtrated supernatant (50 μg) was incubated with 2 mM TFM-01, OB-01 (see Supplementary Fig. 1) or dimethyl sulphoxide (DMSO) at 37 °C for 2 h. The reaction was terminated by adding 10 times volume of methanol. TFM and 2-oxobutyrate were quantified by CE-TOFMS [11] in cationic and anionic mode, respectively, under conditions described previously [11]. TFM and sodium 2-oxobutyrate were used as standards.

2.6. Evaluation of the amoebicidal activity of trifluoromethionine derivatives using a hamster liver abscess model

Approximately 1×10^6 trophozoites were injected into the left lobe of the liver of 2–3-week-old Syrian hamsters (mean ± standard error body weight, 39.9 ± 0.56 g). TFM or its derivatives dissolved in DMSO were administered either subcutaneously (0.1 mL, 0.2 μmol/animal) or orally through a stomach catheter (0.5 mL, 0.2–1.0 μmol/animal) at 24 h after infection. Animals were sacrificed 6 days post infection and the liver and abscesses were dissected and weighed separately.

3. Results and discussion

The in vitro cytotoxicities of TFM, 15 TFM derivatives and 4 control compounds lacking fluorine were evaluated by measuring their 50% inhibitory concentration (IC_{50}) values against *E. histolytica* trophozoites (Table 1). Whilst TFM showed an IC_{50} of 7.34 μM, the derivatives TFM-01 and TFM-02 had IC_{50} values of 2.22–2.28 μM. Three difluoroanilide compounds [2,3-difluoroanilide (TFM-03), 2,6-difluoroanilide (TFM-04) and 2,5-difluoroanilide (TFM-05)] also had a comparable 2.5–3.0-fold reduction in their IC_{50} values compared with TFM. Three derivatives with 2,5- and 3,4-dimethoxyanilide (TFM-07 and TFM-08) or 3,4,5-trimethoxyanilide (TFM-09) modification had a further 2-fold improvement in their IC_{50} values. These values are 1.6–4.3-fold lower than metronidazole (mean ± standard deviation in triplicate, 4.76 μM ± 0.22). In contrast, compounds containing additional functional groups on the phenyl ring of TFM-01 [2-methyl-4-chloroanilide (TFM-10), 2-methoxy-4-bromoanilide (TFM-11), 2-methoxyl-4-chloro-5-methylaniline (TFM-12)] or bulkier structures such as 8-aminoquinoline (TFM-13), 5,6,7,8,-tetrahydro-1-naphthalenamine (TFM-14) and 4-bromo-naphthalenamide (TFM-15) had higher IC_{50} values compared with TFM. The IC_{50} values of TFM-10 and TFM-15 were >80 μM, indicating a loss of efficacy in these derivatives. Furthermore, structurally similar derivatives, in which the trifluoromethyl group was substituted by a methyl group (MET-01 or MET-09), failed to produce cytotoxic activity (IC_{50} >80 μM). These results indicate that the trifluoromethyl group at the C_5-carbon of TFM and its derivatives is essential for their cytotoxicity.

To determine whether α-keto acids generated by the release of trifluoromethane thiol from the TFM derivatives is responsible for their cytotoxic activity, OB-01 and OB-09, which were predicted products of TFM-01 and TFM-09, respectively, were evaluated. Neither OB-01 nor OB-09 showed cytotoxic activity (IC_{50} >80 μM). These results confirmed that the trifluoromethyl group is responsible for the cytotoxicity of TFM and its derivatives [7–9].

To assess whether TFM derivatives were selective towards *E. histolytica*, the efficacy of TFM, TFM-01 and TFM-02 against a representative mammalian cell line was examined. The IC_{50} values of TFM, TFM-01 and TFM-02 against CHO cells were more than 100-times higher than for *E. histolytica* (709 ± 172, 982 ± 174 and 878 ± 149 μM, respectively), whilst those of difluoroanilide and dimethoxyanilide derivatives were higher or slightly lower (>1 mM and 554 ± 94 μM, respectively). It was also previously reported that a high concentration of TFM (100 μg/mL, corresponding to 493 μM) inhibited the growth of mouse myeloma cells [8]. Taken together, TFM and its derivatives have good selectivity toward *E. histolytica*.

To determine whether the observed increase in the cytotoxic effects of the amidated TFM derivatives compared with TFM was due to their higher degradation efficiencies by MGL, time kinetics of the degradation of TFM, TFM-01 and TFM-02 by two recombinant MGL proteins (MGL1 and MGL2) were investigated [5]. Trifluoromethane thiol generated from TFM by MGL1 or MGL2 increased with incubation time (Fig. 1). Degradation of TFM by MGL2 was ca. 12.5-fold faster compared with MGL1 at 10 min after incubation, which is also consistent with a previous study [5]. In contrast, decomposition of TFM-01 and TFM-02 by MGL1 and of TFM-02 by MGL2 was negligible, whilst that of TFM-01 by MGL2 was ca. 70% slower compared with TFM.

We further examined the degradation process of TFM-01 in the amoeba by directly measuring the products formed when

Please cite this article in press as: Sato D, et al. Cytotoxic effect of amide derivatives of trifluoromethionine against the enteric protozoan parasite *Entamoeba histolytica*. Int J Antimicrob Agents (2009), doi:10.1016/j.ijantimicag.2009.08.016

Table 1
Structures and IC_{50} values of TFM and its derivatives against *E. histolytica* in vitro.

Compound name	Structure	IC_{50} (μM) (mean ± S.D.)
TFM	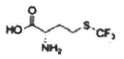	7.34 ± 0.59
TFM-01	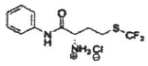	2.22* ± 0.02
TFM-02	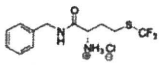	2.28* ± 0.05
TFM-03	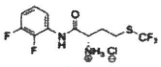	2.37* ± 0.01
TFM-04	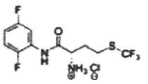	2.97* ± 0.02
TFM-05	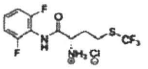	2.46* ± 0.01
TFM-06	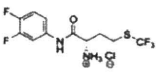	6.66* ± 0.16
TFM-07	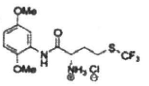	1.11* ± 0.02
TFM-08	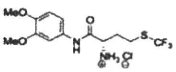	1.19* ± 0.01
TFM-09	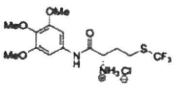	1.28* ± 0.05
TFM-10	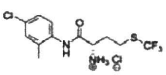	>80
TFM-11	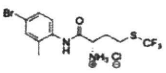	16.86* ± 0.54
TFM-12	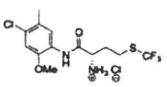	10.02 ± 0.06
TFM-13	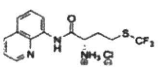	12.48 ± 0.02
TFM-14	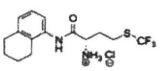	11.58 ± 0.17
TFM-15	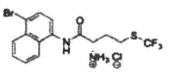	>80
MET-01	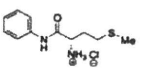	>80
MET-09	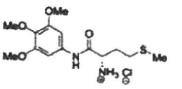	>80
OB-01	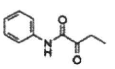	>80
OB-09	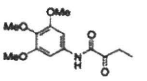	>80

Table 1 (*Continued*)

Compound name	Structure	IC_{50} (μM) (mean ± S.D.)
MNZ	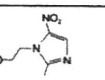	4.76* ± 0.22

* *P* values <0.05 as compared to TFM.

TFM-01 was mixed with the amoebic cell lysate. TFM, TFM-01 and OB-01 were unequivocally quantified on CE-TOFMS (Fig. 2). TFM was detected in the reaction mixture at 10 min and later after the parasite lysate was mixed with TFM-01 (Fig. 2B, solid line). The concentration of TFM detected corresponded to ca. 1% of the initial TFM-01 concentration (2 mM) and did not change after further incubation. The 2-oxobutyrate detected in the reaction mixture increased during the incubation time in a linear fashion, suggestive of continuous hydrolysis and decomposition of TFM-01 that leads to 2-oxobutyrate formation (Fig. 2B, broken line). Neither TFM nor 2-oxobutyrate was detected when the cell lysate was mixed with OB-01 (data not shown). The TFM derivatives containing piperidine, pyrrolidine or morpholine linked to the C_1-carbon (without the amide bond) showed no amoebicidal activity (data not shown). These data suggest that hydrolysis of the TFM derivatives is essential for amoebicidal activity.

To confirm whether the peptidases are involved in the hydrolysis of TFM-01, the cell lysate was pre-incubated with 0.1 mM *N*-[*N*-(L-3-*trans*-carboxirane-2-carbonyl)-L-leucyl]-agmatine (E-64) or 10 mM ethylene diamine tetra-acetic acid (EDTA), respectively. These protease inhibitors reduced decomposition of TFM-01 by ca. 60% and 35%, respectively (data not shown),

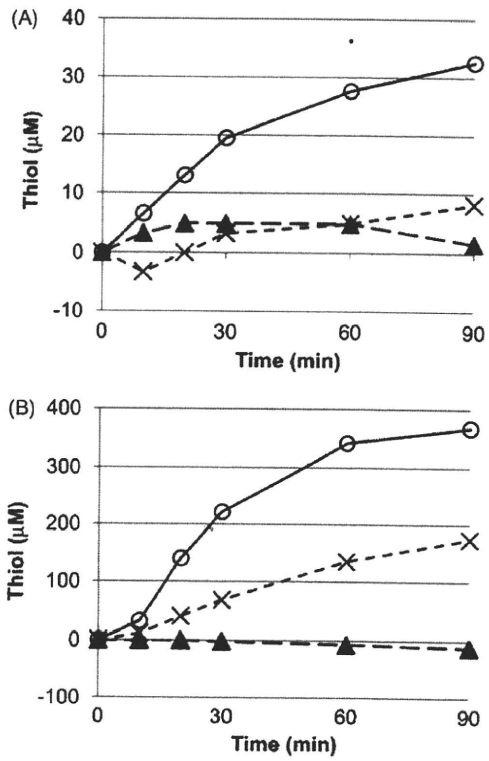

Fig. 1. Time kinetics of the degradation of trifluoromethionine (TFM) and two derivatives [anilide (TFM-01) and benzylamide (TFM-02)] by recombinant L-methionine γ-lyase (MGL). TFM (○), TFM-01 (×) and TFM-02 (▲) were incubated with (A) MGL1 or (B) MGL2 and released thiols were measured as described in Section 2.4.

Please cite this article in press as: Sato D, et al. Cytotoxic effect of amide derivatives of trifluoromethionine against the enteric protozoan parasite *Entamoeba histolytica*. Int J Antimicrob Agents (2009), doi:10.1016/j.ijantimicag.2009.08.016

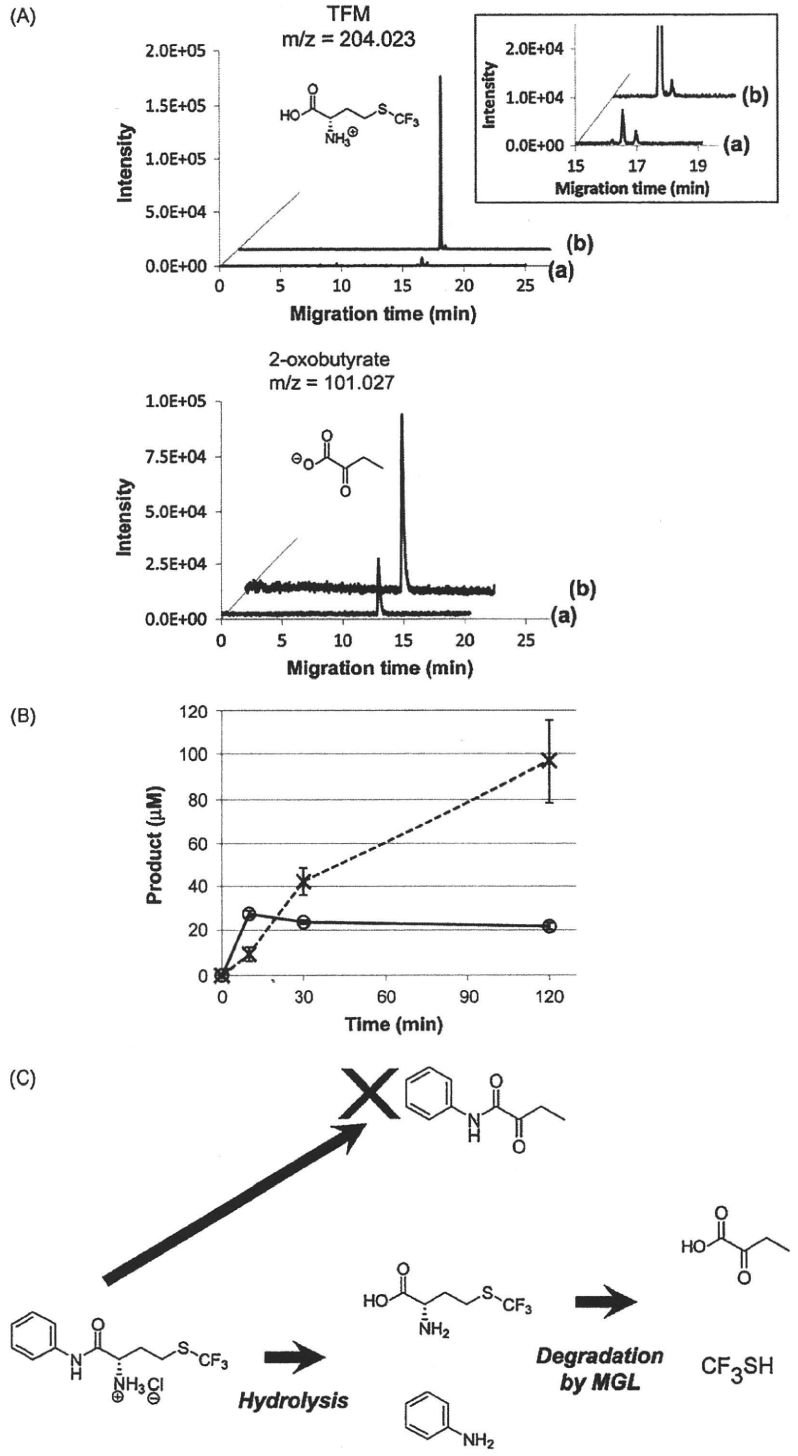

Fig. 2. Time kinetics of trifluoromethionine (TFM) derivative degradation by the amoebic cell lysate. (A) Identification and quantification of TFM and 2-oxobutyrate. Representative electropherograms of TFM (upper panel; a magnified figure is also shown in the inset) and 2-oxobutyrate (lower panel) of TFM-01 incubated with (a) the cell lysate at 37 °C for 2 h and (b) the standard (100 μM). (B) The amoebic cell lysate (50 μg) was incubated with 2 mM TFM-01 or 5% dimethyl sulphoxide (DMSO) (control) for the indicated times. The concentration of TFM (○) and 2-oxobutyrate (×) was quantified by capillary electrophoresis with electrospray ionisation time-of-flight mass spectrometry (CE-TOFMS). Data shown are mean ± standard deviation in triplicate. (C) A proposed scheme for TFM-01 degradation in *Entamoeba histolytica*. MGL, L-methionine γ-lyase.

suggesting that cysteine proteases and metalloproteases participate in the hydrolysis of TFM derivatives in *E. histolytica*. It is conceivable to assume that TFM is incorporated into the amoebae by amino acid transporter(s). It has also been reported that the parasite incorporates amino acids directly from the culture medium [12]. However, it remains to be clarified whether the TFM derivatives are incorporated via the presumed amino acid transporter(s) or by passive diffusion due to their hydrophobic nature.

The amoebicidal activity of the 16 compounds containing the trifluoromethyl group was evaluated using a hamster liver

Please cite this article in press as: Sato D, et al. Cytotoxic effect of amide derivatives of trifluoromethionine against the enteric protozoan parasite *Entamoeba histolytica*. Int J Antimicrob Agents (2009), doi:10.1016/j.ijantimicag.2009.08.016

Table 2
Amoebicidal activity of trifluoromethionine (TFM) derivatives by subcutaneous administration in a hamster amoebic liver abscess model.

Compound name	Increase in body weight (%) (mean ± S.E.)[a]	Weight of abscess (%) (mean ± S.E.)[b]	Number of animals
TFM	22.9 ± 12.8	24.5 ± 14.8	3
TFM-01	13.4 ± 0.5	29.1 ± 5.2	2
TFM-02	41.2 ± 4.3	17.9 ± 1.1	3
TFM-03	26.6 ± 2.9	32.6 ± 1.7	3
TFM-04	27.7 ± 3.4	30.3 ± 7.5	3
TFM-05	25.1 ± 2.8	15.4 ± 5.1	3
TFM-06	45.8 ± 10.6	17.7 ± 0.8	3
TFM-07	30.9 ± 2.6	15.3 ± 5.6	2
TFM-08	19.1 ± 7.2	0.2 ± 0.2	3
TFM-09	4.3 ± 4.3	8.2 ± 7.9	3
TFM-10	7.9 ± 7.9	0.2 ± 0.1	3
TFM-11	0.4 ± 0.2	19.4 ± 5.6	3
TFM-12	0.2 ± 0.2	3.2 ± 1.5	3
TFM-13	26.7 ± 13.6	5.4 ± 5.2	3
TFM-14	24.6 ± 6.3	5.6 ± 5.6	3
TFM-15	3.5 ± 0.8	0.0 ± 0.0	3
Control[c]	26.5 ± 9.0	39.7 ± 1.8	3

[a] Percentage increase in body weight between Days 0 and 6.
[b] Percentage of the abscess relative to the weight of the liver.
[c] DMSO (100 μL/head).

abscess model (Table 2). Trophozoites were directly injected into the liver and 24 h later 0.2 μmol of TFM or its derivatives were subcutaneously injected into the hamsters. Two difluoroanilide derivatives (TFM-04 and TFM-05), one dimethoxyanilide (TFM-07) and 5,6,7,8-tetrahydro-1-naphthylamide compound (TFM-14) exhibited antiamoebic effects comparable with that of TFM. All the other compounds except for TFM-06, TFM-09, TFM-11 and TFM-15 also showed comparable or slightly lower efficacy compared with TFM. It is also worth noting that the hamsters treated with TFM-04, TFM-07 or TFM-14 gained more weight compared with the other effective compounds.

Next we evaluated the in vivo efficacy of TFM-14, which showed the highest efficacy by subcutaneous administration, and TFM via oral administration (Table 3). Single oral administration of TFM at 2.54 mg/kg (0.5 μmol/animal equivalent) completely prevented liver abscess formation; TFM-14 had comparable or slightly lower potency compared with TFM [100% cure with 9.22 mg/kg (1.0 μmol/animal equivalent)]. Pargal et al. [13] showed that only 19 of 29 animals receiving 100 mg/kg (ca. 30 μmol/animal) oral metronidazole were cured of amoebic liver abscesses. Although we may not be able to compare directly their data [13] with ours because of subtle differences in experimental conditions, TFM and TFM-14 are likely to be more effective in preventing the formation of amoebic liver abscesses than metronidazole in the hamster model.

Table 3
Amoebicidal activity of trifluoromethionine (TFM) derivatives by oral administration in a hamster amoebic liver abscess model.

Compound name	Dose (mg/kg)	Increase in body weight (%) (mean ± S.E.)[a]	Weight of abscess (%) (mean ± S.E.)[b]	Number of animals
TFM	1.02	35.1 ± 2.1	7.8 ± 5.9	3
	2.54	27.6 ± 4.5	0.0 ± 0.0	3
	3.56	34.5 ± 2.2	1.7 ± 1.4	3
	5.08	27.7 ± 5.9	0.0 ± 0.0	3
TFM-14	1.84	26.3 ± 3.2	30.2 ± 1.7	3
	4.61	23.3 ± 8.3	11.3 ± 9.2	3
	6.45	22.4 ± 2.9	3.9 ± 2.5	3
	9.22	33.9 ± 3.7	0.0 ± 0.0	3
Control[c]		5.0 ± 0.9	47.6 ± 0.0	2

[a] Percentage increase in body weight between Days 0 and 6.
[b] Percentage of the abscess relative to the weight of the liver.
[c] DMSO (100 μL/head).

We have previously shown that the carbonothionic difluoride derived from TFM degradation by MGL non-specifically cross-links the primary amino group of MGL and other proteins in vitro and is responsible for the cytotoxicity of TFM [5]. Since the target of carbonothionic difluoride is non-specific and is not limited to the targets of 5-nitroimidazoles, such as pyruvate:ferredoxin oxidoreductase, thioredoxin reductase and nitroreductase [14–16], TFM and its derivatives are expected to be effective against 5′-nitroimidazole-resistant *E. histolytica* [17], *T. vaginalis* [18], periodontal bacteria and *Citrobacter freundii*.

Acknowledgments

The authors thank Rumiko Kosugi (Department of Parasitology, Gunma University Graduate School of Medicine, Gunma, Japan) for technical assistance. They also thank Mr Yuji Kakazu and Mr Akiyoshi Hirayama (Institute for Advanced Biosciences, Keio University, Yamagata, Japan) for technical help with mass spectrometry.

Funding: This work was supported by a Grant-in-Aid for Scientific Research from the Ministry of Education, Culture, Sports, Science and Technology of Japan to DS (20590429) and TN (18GS0314, 18050006 and 18073001), a grant for research on emerging and re-emerging infectious diseases from the Ministry of Health, Labour and Welfare of Japan, and a grant for research to promote the development of anti-AIDS pharmaceuticals from the Japan Health Sciences Foundation to TN.

Competing interests: None declared.

Ethical approval: Not required.

Appendix A. Supplementary data

Supplementary data associated with this article can be found, in the online version, at doi:10.1016/j.ijantimicag.2009.08.016.

References

[1] Ali V, Nozaki T. Current therapeutics, their problems, and sulfur-containing-amino-acid metabolism as a novel target against infections by "amitochondriate" protozoan parasites. Clin Microbiol Rev 2007;20:164–87.
[2] Freeman CD, Klutman NE, Lamp KC. Metronidazole. A therapeutic review and update. Drugs 1997;54:679–708.
[3] Wassmann C, Hellberg A, Tannich E, Bruchhaus I. Metronidazole resistance in the protozoan parasite *Entamoeba histolytica* is associated with increased expression of iron-containing superoxide dismutase and peroxiredoxin and decreased expression of ferredoxin 1 and flavin reductase. J Biol Chem 1999;274:26051–6.
[4] Tanaka H, Esaki N, Soda K. A versatile bacterial enzyme: L-methionine γ-lyase. Enzyme Microb Technol 1985;7:530–7.
[5] Sato D, Yamagata W, Harada S, Nozaki T. Kinetic characterization of methionine γ-lyases from the enteric protozoan parasite *Entamoeba histolytica* against physiological substrates and trifluoromethionine, a promising lead compound against amoebiasis. FEBS J 2008;275:548–60.
[6] Zygmunt WA, Tavormina PA. DL-*S*-Trifluoromethylhomocysteine, a novel inhibitor of microbial growth. Can J Microbiol 1966;12:143–8.
[7] Yoshimura M, Nakano Y, Koga T. L-Methionine-γ-lyase, as a target to inhibit malodorous bacterial growth by trifluoromethionine. Biochem Biophys Res Commun 2002;292:964–8.
[8] Coombs GH, Mottram JC. Trifluoromethionine, a prodrug designed against methionine γ-lyase-containing pathogens, has efficacy in vitro and in vivo against *Trichomonas vaginalis*. Antimicrob Agents Chemother 2001;45:1743–5.
[9] Tokoro M, Asai T, Kobayashi S, Takeuchi T, Nozaki T. Identification and characterization of two isoenzymes of methionine γ-lyase from *Entamoeba histolytica*: a key enzyme of sulfur-amino acid degradation in an anaerobic parasitic protist that lacks forward and reverse trans-sulfuration pathways. J Biol Chem 2003;278:42717–27.
[10] Clark CG, Diamond LS. Methods for cultivation of luminal parasitic protists of clinical importance. Clin Microbiol Rev 2002;15:329–41.
[11] Hirayama A, Kami K, Sugimoto M, Sugawara M, Toki N, Onozuka H, et al. Quantitative metabolome profiling of colon and stomach cancer microenvironment by capillary electrophoresis time-of-flight mass spectrometry. Cancer Res 2009;69:4918–25.
[12] Zuo X, Coombs GH. Amino acid consumption by the parasitic, amoeboid protists *Entamoeba histolytica* and *E. invadens*. FEMS Microbiol Lett 1995;130:253–8.

Please cite this article in press as: Sato D, et al. Cytotoxic effect of amide derivatives of trifluoromethionine against the enteric protozoan parasite *Entamoeba histolytica*. Int J Antimicrob Agents (2009), doi:10.1016/j.ijantimicag.2009.08.016

[13] Pargal A, Rao C, Bhopale KK, Pradhan KS, Masani KB, Kaul C. Comparative pharmacokinetics and amoebicidal activity of metronidazole and satranidazole in the golden hamster, *Mesocricetus auratus*. J Antimicrob Chemother 1993;32:483–9.
[14] Leitsch D, Kolarich D, Wilson IB, Altmann F, Duchêne M. Nitroimidazole action in *Entamoeba histolytica*: a central role for thioredoxin reductase. PLoS Biol 2007;5:e211.
[15] Pal D, Banerjee S, Cui J, Schwartz A, Ghosh SK, Samuelson J. *Giardia*, *Entamoeba*, and *Trichomonas* enzymes activate metronidazole (nitroreductases) and inactivate metronidazole (nitroimidazole reductases). Antimicrob Agents Chemother 2009;53:458–64.
[16] Samuelson J. Why metronidazole is active against both bacteria and parasites. Antimicrob Agents Chemother 1999;43:1533–41.
[17] Samarawickrema NA, Brown DM, Upcroft JA, Thammapalerd N, Upcroft P. Involvement of superoxide dismutase and pyruvate:ferredoxin oxidoreductase in mechanisms of metronidazole resistance in *Entamoeba histolytica*. J Antimicrob Chemother 1997;40:833–40.
[18] Upcroft JA, Upcroft P. Drug susceptibility testing of anaerobic protozoa. Antimicrob Agents Chemother 2001;45:1810–4.

Please cite this article in press as: Sato D, et al. Cytotoxic effect of amide derivatives of trifluoromethionine against the enteric protozoan parasite *Entamoeba histolytica*. Int J Antimicrob Agents (2009), doi:10.1016/j.ijantimicag.2009.08.016

Parasitology International 59 (2010) 75–81

Contents lists available at ScienceDirect

Parasitology International

journal homepage: www.elsevier.com/locate/parint

Identification of an avirulent *Entamoeba histolytica* strain with unique tRNA-linked short tandem repeat markers

Aleyla Escueta-de Cadiz [a,b], Seiki Kobayashi [c], Tsutomu Takeuchi [c], Hiroshi Tachibana [d], Tomoyoshi Nozaki [a,*]

[a] Department of Parasitology, National Institute of Infectious Diseases, 1-23-1 Toyama, Shinjuku-ku, Tokyo 162-8640, Japan
[b] Department of Parasitology, Gunma University Graduate School of Medicine, 3-39-22 Showa-machi, Maebashi, Gunma 371-8511, Japan
[c] Department of Tropical Medicine and Parasitology, Keio University School of Medicine, 35 Shinanomachi, Shinjuku-ku, Tokyo 160-8582, Japan
[d] Department of Infectious Diseases, Tokai University School of Medicine, Isehara, Kanagawa 259-1193, Japan

ARTICLE INFO

Article history:
Received 21 July 2009
Received in revised form 29 October 2009
Accepted 29 October 2009
Available online 4 November 2009

Keywords:
Amebiasis
Short tandem repeat
tRNA
Virulence
Symptomatic
Asymptomatic

ABSTRACT

Highly polymorphic, non-coding short tandem repeats (STR) are scattered between the tRNA genes in *Entamoeba histolytica* in a unique tandemly arrayed organization. STR markers that correlate with the virulence of individual *E. histolytica* strains have recently been reported. Here we evaluated the usefulness of tRNA-linked STR loci as genetic markers in identifying virulent and avirulent strains of *E. histolytica* from 37 Japanese *E. histolytica* samples (12 diarrheic/dysenteric, 20 amebic liver abscess (ALA), and 5 asymptomatic cases). Twenty three genotypes, assigned by combining the STR sequence types from all 6 STR loci, were identified. One to 8 new STR sequence types per locus were also discovered. Genotypes found in asymptomatic isolates were highly polymorphic (4 out of 5 genotypes were unique to this group), while in symptomatic isolates, almost half of the genotypes were shared between diarrhea/dysentery and ALA. One asymptomatic isolate (KU27) showed unique STR patterns in 4 loci. This strain, though associated with the typical pathogenic zymodeme II, failed to induce amebic liver abscess by animal challenge, which suggests that inherently avirulent *E. histolytica* strains exist, that are associated with unique genotypes. Furthermore, STR genotyping and *in vivo* challenge of 2 other asymptomatic isolates (KU14 and KU26) verified the covert virulence of these strains.

1. Introduction

Amebiasis, caused by the anaerobic/microaerophilic protozoan parasite *Entamoeba histolytica*, ranges from the asymptomatic carrier state, where patients do not show any characteristic signs of infection and microscopic stool examination often reveals the dormant cyst form, to the symptomatic state, where trophozoites damage the intestinal epithelium and cause diarrhea, colitis, and dysentery. In 5–20% of the patients with intestinal symptoms, trophozoites spread to extraintestinal organs such as the liver, lungs, and brain. The amebic liver abscess is the most common form of extraintestinal amebiasis [1,2].

What determines the outcome of infection remains to be answered. It has been shown that host immune mechanisms such as cytokines and interleukins play crucial roles in preventing or delaying tissue invasion, and specific human leukocyte antigen class II alleles have been demonstrated to reduce susceptibility to amebic infection [1,3]. On the other hand, although genetic polymorphism in *E. histolytica* isolates is well established and several polymorphic markers including the serine-rich *E. histolytica* protein (SREHP), chitinase, and repeat containing loci 1–2 and 5–6 were reported [4–9], a link between a genotype and the outcome of infection has not been demonstrated until recently [10,11].

Recent disclosure of the genome sequence of *E. histolytica* HM-1: IMSS strain [12] elucidated various unique features of the genome structure of this parasite [13]. One important finding is the presence of 4500 tandemly arrayed tRNA genes. Twenty five tRNA array units contain 1 to 5 tRNA genes which are adjoined to STRs [10]. A previous study showed that a high degree of polymorphism in these tRNA-linked STRs are observed in the early branching *E. histolytica* and its non-pathogenic sibling *Entamoeba dispar* [14]. STRs are DNA sequences of about 2 to 8 base pairs that are repeated up to 40 times in a head-to-tail manner. Currently, STR typing is widely used in paternity testing and forensic cases because the number of copies of repeats varies among individuals. A recent study indicated that *E. histolytica* tRNA-linked STRs were useful to establish a correlation between the genotype of the parasite, based on the size of the PCR-amplified fragment, and the outcome of infection [10,11]. However, a correlation remains to be established clearly at the nucleotide level between the polymorphic markers and the clinical symptoms.

Abbreviation: STR, short tandem repeat.

* Corresponding author. Tel.: +81 3 5285 1111x2600; fax: +81 327 5285 1219.
E-mail address: nozaki@nih.go.jp (T. Nozaki).

1383-5769/$ – see front matter © 2009 Published by Elsevier Ireland Ltd.
doi:10.1016/j.parint.2009.10.010

Furthermore, the potential of these tRNA-linked STRs as a marker for avirulence is not well studied.

In Japan, amebiasis is usually seen within restricted social populations such as the mentally handicapped and men who have sex with men (MSM) [7,8,15]. Epidemiological data show that the number of cases has increased from 2003 to 2007, and a higher number of cases are now also seen among female sexual workers [16]. We previously showed that extensive genetic polymorphism at SREHP, chitinase, and 2 tRNA-linked STRs (loci 1–2 and 5–6) exist in Japanese *E. histolytica* strains isolated from patients who have no history of traveling abroad [7,8]. In this study, the usefulness of 6 tRNA-linked STR loci as genetic markers has been evaluated in 37 Japanese *E. histolytica* samples, to differentiate the genotypes associated with severe or asymptomatic cases of amebiasis, although the conclusions drawn from this study may be restricted to the geographic origins where these isolates were derived from. Furthermore, we also described a unique genotype and 4 STR types, which can be used to identify potentially avirulent strains of *E. histolytica*.

2. Materials and methods

2.1. Clinical samples and cultivation

A total of 37 Japanese *E. histolytica* samples (Table 1) were included in this study (12 diarrheic/dysenteric, 20 amebic liver abscess, and 5 asymptomatic cases). Fifteen isolates which were previously described [7,8], were collected from mentally handicapped and MSM patients. Since the genotypes of isolates obtained from the mentally handicapped patients were identical within each institution [7,8], only 3 representative isolates (KU14, 26, and 27) were chosen. These isolates were recovered from liquid nitrogen and cultured either in xenic condition using Robinson's medium [17] or in monoxenic condition using yeast extract–iron–maltose–dihydroxyacetone-serum (YIMDHA-S) medium supplemented with *Crithidia fasciculata* [18,19]. Five new clinical isolates also maintained in YIMDHA-S, were obtained from Keio University School of Medicine. DNA samples was also extracted from 17 liver abscess specimens.

2.2. Polymerase chain reaction (PCR) and DNA sequencing

Total DNA from the xenic and monoxenic cultures was extracted using QIAamp DNA stool minikit (Qiagen, Tokyo, Japan), whereas the DNAs from ALA patients were extracted directly from abscess samples using the conventional methods as previously described [20]. The STR fragments were amplified using 6 *E. histolytica*-specific tRNA-linked STR primers (DA-H, AL-H, NK2-H, RR-H, SQ-H, and S^{TGA}D-H) under the conditions previously described [21]. The amplified PCR products were separated using 1.5% agarose gel (Takara, Japan) and purified using phenol/chloroform and ethanol precipitation. Sequence analysis was performed using the forward or reverse *E. histolytica*-specific tRNA-linked STR primers [21] and BigDye® Terminator v.3.1 cycle sequencing kit (Applied Biosystems, Foster City, CA). An illustra MicroSpin G-50 column (GE Healthcare, UK) was used for purifying labeled DNA from unincorporated labeled nucleotides. Sequencing was performed on an ABI PRISM 310 Genetic Analyzer. Nucleotide sequences were analyzed using the Tandem Repeats Finder software to identify the STRs [22]. Newly identified STR patterns discovered in Japanese *E. histolytica* samples were submitted to GenBank/EMBL/DDBJ database with accession numbers AB457150–AB457168.

2.3. Animal challenge with clinical isolates

Representative asymptomatic isolates (KU14, KU26 and KU27) from 3 mental institutions and the HM-1:IMSS clone 6 (HM-1) strain used as a positive control, were included in this experiment. The clinical isolates were cultured monoxenically in YIMDHA-S medium supplemented with *C. fasciculata*, while HM-1 was axenically maintained in a BI-S-33 medium. Approximately 1×10^6 trophozoites of KU14, KU26, and HM-1, harvested at the late logarithmic phase of growth, were suspended in phosphate buffer saline and directly inoculated into the left liver lobe of 3–4 week-old Syrian golden hamsters (40–50 g; 5 hamsters/strain), while $1–2 \times 10^6$ trophozoites were used for KU27. After 6 days of infection, the hamsters were sacrificed and the liver and amebic liver abscesses were dissected and weighed. The hamsters used in the experiment were not tested for antibodies against *E. histolytica*, as antibody production is not observed at 6 days of infection (S. Kobayashi, unpublished).

Table 1
Background of the Japanese *E. histolytica* samples used in this study.

No.	Isolate[a]	Clinical diagnosis	Isolation		DNA origin
			Location	Date	
1	KU 5	Asymptomatic	Tokyo	Nov 1988	Monoxenic
2	KU 14	Asymptomatic	Okayama (Institution)	Nov 1999	Xenic
3	KU 26	Asymptomatic	Shizuoka (Institution)	Sept 2000	Monoxenic
4	KU 27	Asymptomatic	Shizuoka (Institution)	Jan 2001	Xenic
5	KU 31	Asymptomatic	Tokyo	March 2001	Xenic
6	KU 1	Diarrhea	Tokyo	July 1994	Xenic
7	KU 2	Diarrhea	Tokyo	Dec 1988	Monoxenic
8	KU 3	Diarrhea	Kyoto	Sept 1988	Monoxenic
9	KU 10	Diarrhea	Tokyo	Oct 1991	Xenic
10	KU 15	Diarrhea	Tokyo	Sept 1994	Xenic
11	KU 16	Diarrhea	Tokyo	May 1993	Xenic
12	KU 23	Diarrhea	Tokyo	Feb 2000	Xenic
13	KU 32	Diarrhea	Tokyo	June 2001	Xenic
14	KU 45	Diarrhea	Chiba	April 2004	Monoxenic
15	KU 46[b]	Diarrhea	Shizuoka	April 2004	Monoxenic
16	KU 47[c]	Diarrhea	Tokyo	April 2004	Monoxenic
17	KU 50	Diarrhea	Tokyo	March 2007	Monoxenic
18	KU 8	ALA	Tokyo	May 1995	Xenic
19	KU 11	ALA	Tokyo	Feb 1994	Xenic
20	KU 48	ALA	Tokyo	May 2006	Monoxenic
21	C726	ALA	Chiba	July 2006	Abscess
22	ALA-1	ALA	Kanagawa	July 1991	Abscess
23	ALA-2	ALA	Tokyo	Nov 1990	Abscess
24	ALA-3	ALA	Ibaraki	Sept 1991	Abscess
25	ALA-4	ALA	Tokyo	Feb 1985	Abscess
26	ALA-5	ALA	Tokyo	Feb 1985	Abscess
27	ALA-6	ALA	Tokyo (Peru?)[d]	Feb 1985	Abscess
28	ALA-7	ALA	Kanagawa	March 1991	Abscess
29	ALA-8	ALA	Kagawa (Europe? Africa?)[d]	March 1991	Abscess
30	ALA-9	ALA	Ehime	Dec 1991	Abscess
31	ALA-10	ALA	Tokyo	March 1993	Abscess
32	ALA-12	ALA	Tokyo	Sept 1993	Abscess
33	ALA-13	ALA	Kanagawa	Oct 1994	Abscess
34	ALA-14	ALA	Kanagawa	June 1995	Abscess
35	ALA-15	ALA	Tokyo	April 1997	Abscess
36	ALA-16	ALA	Kanagawa	Feb 1998	Abscess
37	ALA-17	ALA	Kanagawa	June 1999	Abscess

[a] Samples 1–13, 18, 19, and 22–30 were used in previous studies (refs. [7,8,20]).
[b] Metronidazole resistant.
[c] HIV positive.
[d] Possible place of infection.

2.4. Statistical analyses

Fischer's exact test was used to evaluate the significance of correlations between the STRs and the genotypes among the different groups of infection outcomes. The mean, standard deviation and *p*-values were calculated using Student's *t*-test to determine the average percentage of abscess per liver.

3. Results and discussion

3.1. STR polymorphisms in the length and nucleotide sequences

We observed that isolates with identical PCR size-based STR types displayed distinct nucleotide sequences. We thus examined the tRNA-linked STRs of 37 Japanese *E. histolytica* samples by direct sequencing since nucleotide sequence-based differentiation of STR types is essential for high resolution typing of clinical isolates [7,8,14]. Fig. 1 shows the agarose gel pattern of 8 representative isolates in 6 loci. Variations in fragment lengths were discernible for loci N-K2, R-R, and S^{TGA}-D, but were obscure for D-A, A-L, and S-Q. Direct sequencing of the amplified STR fragments clarified this obscurity, as previously shown [14]. The STRs amplified from the samples revealed 9 STR variations in the A-L locus, 8 in N-K2, 6 in D-A and R-R loci, and 5 in S^{TGA}-D and S-Q loci (Fig. 2). Uniformity in length and sequence pattern was observed in D-A (Fig. 1A, lanes 4–8; Fig. 2A, 5DA), A-L (Fig. 1B, lanes 4, and 6–8; Fig. 2B, 4AL), and N-K2 loci (Fig. 1C, lanes 4, 7, and 11; Fig. 2C, 10NK). Although the size of the amplified products was similar in the R–R (Fig. 1D, lanes 5 and 9–11) and SQ loci (Fig. 1F, lanes 4–8 and 11), their corresponding nucleotide sequences were often distinct (Fig. 2D, 2RR/5RR; Fig. 2F, 4SQ/J4SQ). All STR types in the S^{TGA}-D locus were diverse both in length and sequence pattern (Fig. 2E). Newly identified sequences have been deposited to GenBank/EMBL/DDBJ database with accession numbers AB457150–AB457168.

3.2. STR types and genotypes of the Japanese E. histolytica strains

A genotype was assigned by combining the STR sequence types obtained from 6 STR loci and a total of 23 genotypes were identified (Table 2 and Fig. 2). The STRs that had been reported previously [14,23] or personally communicated by Dr. C. Graham Clark, London School of Hygiene and Tropical Medicine, were named according to his nomenclature, and newly identified sequence types and genotypes were assigned alphanumerical codes beginning with the letter "J" to indicate their Japanese origin.

3.2.1. Asymptomatic isolates

Of the 5 genotypes assigned to the asymptomatic group, 4 (J2 to J5) were unique to the group. Genotype J1 (KU5) was shared with the symptomatic isolates, while genotype J5 (KU31) was also similar (identical for 5 of 6 loci) to those of two ALA isolates (ALA-7 and ALA-12). KU5 and KU31 were obtained from MSM patients visiting an outpatient clinic, where they were clinically diagnosed as asymptomatic cases but were serologically positive [8]. This suggests that despite the

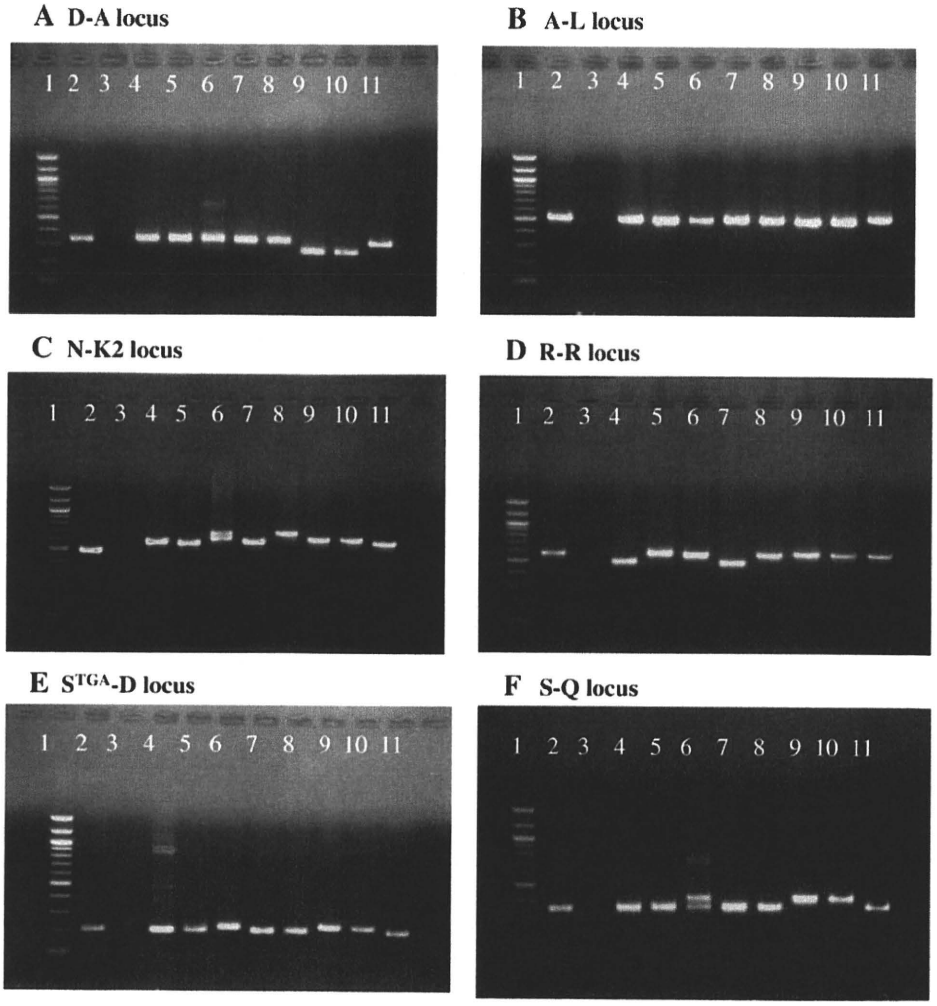

Fig. 1. Fragment length polymorphisms of 8 representative isolates in 6 tRNA-linked STR arrays. Lane 1 corresponds to the 100 bp DNA marker. Lanes 2 and 3 correspond to the reference HM-1:IMSS strain and "no template" negative control, respectively. Lanes 4 and 5 correspond to asymptomatic isolates KU5 and KU14; lanes 6–9 and 11 are isolates KU2, KU3, KU46, KU45, and KU47 from diarrheic patients; lane 10 is KU48 isolate from an ALA case. The number of the STR repeats affects variation in the size of the whole fragment that contains both non-repeat and repeat regions.

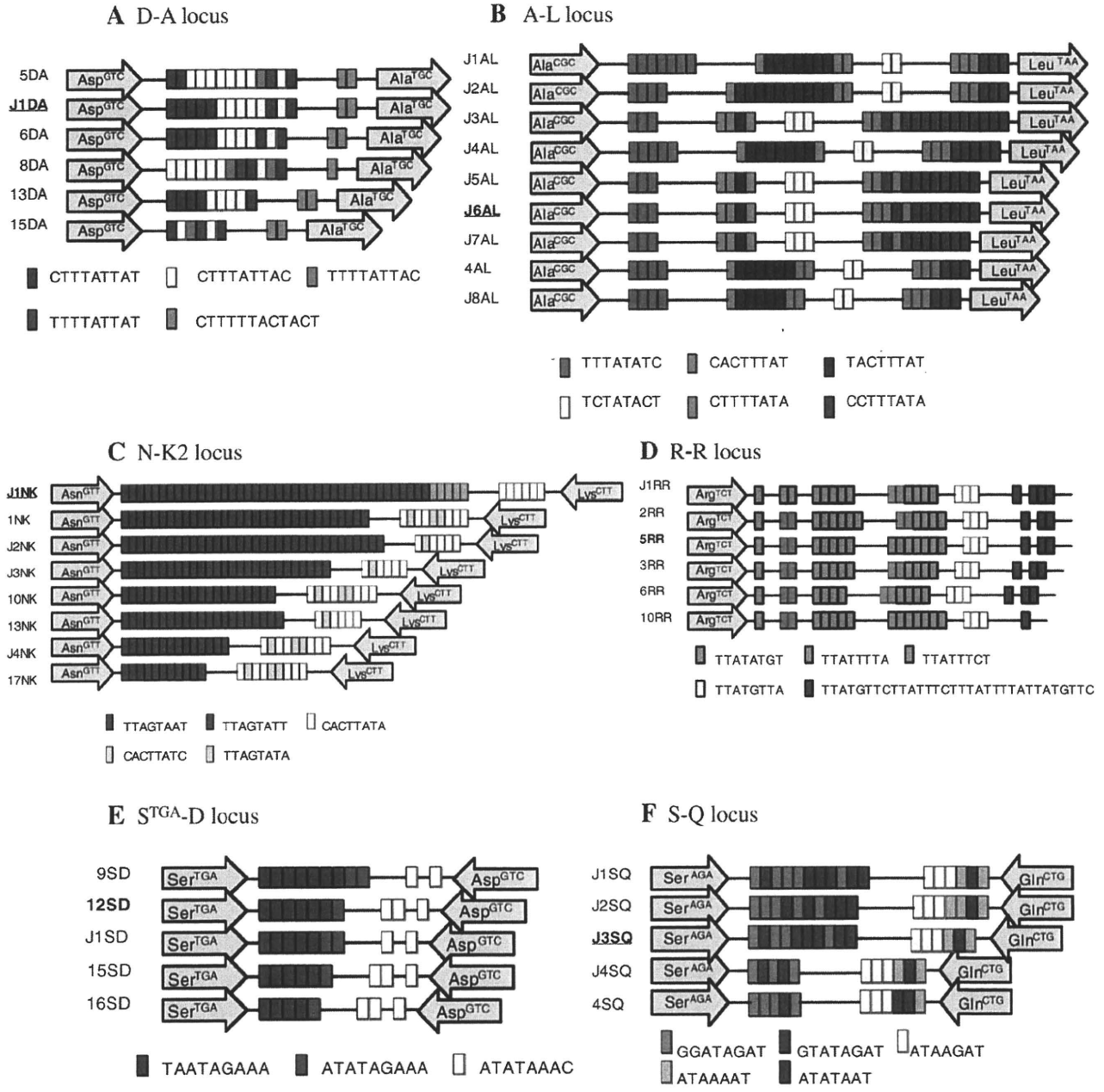

Fig. 2. Schematic representation of STR types of each loci based on the nucleotide sequence of isolates found in this study. tRNA genes and STRs are depicted in arrows and rectangles, respectively, while non-tRNA, non-STR regions are shown in lines. The 6 STR sequence types for isolate KU27 are shown in bold and the 4 STR sequence types that are unique to this isolate are underlined. The schematic diagrams of the D-A, A-L and S-Q loci were personally communicated by Dr. C. Graham Clark.

absence of symptoms invasion could be present. This premise is supported by reports of amebic colitis diagnosed through colonoscopy in asymptomatic homosexual and heterosexual Japanese patients. These patients had no gastrointestinal symptoms but had minute intestinal ulcerations containing *E. histolytica* trophozoites [24,25], which indicates that certain strains might not elicit symptoms even after tissue invasion. Thus, STR type-based genotyping may help in identifying such occult cases among asymptomatic patients.

The STR patterns of genotypes J2 and J3 (KU14 and KU26) were distinct from those in the symptomatic groups in 2 loci, while the STR patterns of the 4 remaining loci overlapped with the symptomatic groups. In contrast, the STR patterns of 4 loci were unique in genotype J4 (KU27). The unique features of the STR types of genotype J4 are discussed below. Genotypes J2 to J4 were seen among isolates from different mental institutions. We chose only one representative asymptomatic isolate each from institutions in the present study, because our previous genotyping of loci 1–2, 5–6, SREHP, and chitinase [7,8] of asymptomatic isolates showed that the genotypes of the isolates from a single institution were identical. However, the better resolution power of the STR-based typing using 6 loci may reveal heterogeneity of the genotypes among isolates from a single institution.